12-2006

Cooling of QPS Modular Coils using Embedded Copper Tubes

Shankar Narasimhaswami
University of Tennessee - Knoxville

To the Graduate Council:

I am submitting herewith a thesis written by Shankar Narasimhaswami entitled "Cooling of QPS Modular Coils using Embedded Copper Tubes." I have examined the final electronic copy of this thesis for form and content and recommend that it be accepted in partial fulfillment of the requirements for the degree of Master of Science, with a major in Mechanical Engineering.

Madhu S. Madhukar, Major Professor

We have read this thesis and recommend its acceptance:

Amold Lumsdaine, Thomas E. Shannon

Accepted for the Council:
Carolyn R. Hodges

Vice Provost and Dean of the Graduate School

(Original signatures are on file with official student records.)

To the Graduate Council:

I am submitting herewith a thesis written by Shankar Narasimhaswami entitled “Cooling of QPS Modular Coils using Embedded Copper Tubes”. I have examined the final electronic copy of this thesis for form and content and recommend that it be accepted in partial fulfillment of the requirements for the degree of Master of Science, with a major in Mechanical Engineering.

Madhu S. Madhukar

Major Professor

We have read this thesis and
recommend its acceptance:

Arnold Lumsdaine

Thomas E. Shannon

Accepted for the Council:

Anne Mayhew

Vice Chancellor and Dean of
Graduate studies

(Original signatures are on file with official student records.)

Cooling of QPS Modular Coils using Embedded Copper Tubes

A Thesis Presented for the
Master of Science
Degree
The University of Tennessee, Knoxville

Shankar Narasimhaswami
December 2006

DEDICATION

This thesis is dedicated to JRD TATA, one of the greatest visionaries and philanthropists I have ever known, to my parents Mr. P Narasimhaswami and Dr. (Mrs.) R Balasaraswathi, to my guide & mentor Dr. Madhu S. Madhukar and to my uncle Mr. R Venkatesan

ACKNOWLEDGMENTS

First I would like to express my deepest gratitude to my guide and mentor Dr. Madhu S. Madhukar without whom I would not have got this excellent opportunity to work with the QPS team in first place and interact with ORNL researchers. It would be undeniably less to just say I am lucky to have worked as his research assistant because he guided me in more than just research.

I am highly indebted to Mr. Paul Goranson without whom it was feeling like 'Rocket science' in carrying out this work. I would really like to recoin it as 'Nuclear science' now. It is his idea that I have extended to my analysis. I thank him for his time, patience and of course his Excel spread sheets with which he introduced the subject to me and helped me throughout.

My sincere thanks to our weekly QPS meeting chair, Dr. Tom Shannon. It was really the discussion and subsequent decisions taken at the meetings, which helped me, plot and replot all my plots. My interactions with him were highly motivating and he used to tell me, "You are in good hands. You are with a good team". I thank him for the constant motivation and support.

I would like to thank Dr. Arnold Lumsdaine for his valuable discussions on my analysis results. His insights into my finite element and analytical models were very helpful in understanding the subject. Besides QPS, I must admit I am a fan for his sense of humor and breadth of English vocabulary and that helped me improve a lot. Thanks much for all that Dr. Lumsdaine.

I would like to thank Dr. Robert Benson for teaching me all about lay-up of the conductor and helping me with any information needed about the project. On a personal note, I would like to thank him for encouraging me throughout my tenure at MDL.

I would like to thank Mr. Jim Lyon for his thoughts and questions on the work I presented at every meeting. These helped me a long way in learning more about any problem and give a thought about the questions and concerns that might arise on any work presented.

I should say it's indeed an honor to have worked with one of the best engineers in this subject, Mr. Brad Nelson. His approach to all my research problems and his interpretation of results helped me a lot in identifying where I was going wrong. I am inspired by his modesty and sound knowledge in all concerned areas. Never did I miss any appreciation for even a small work and that encouraged me to churn out more. Thank you very much Sir.

I would like to thank Mr. Paul Fogarty for all the comments during my presentations.

I would like to specially thank Mr. Kevin Freudenberg for helping me prepare for SOFE conference and for all the discussions I had about my work since the beginning of the project. His speedy 'back paper' calculations were very helpful.

Special thanks to Mr. Joe Campbell for helping in studies relating to flushing the copper tube and also for teaching little magic.

This list would never be complete without expressing my heartfelt thanks to my beloved friends VPD Harisudhakar, Eric Pius Pradeep, Sri Harish Valluru and Suman Duvvuru who have made every single day of my stay in the United States a very pleasant and exhilarating one.

ABSTRACT

In an era of insatiable appetite for energy, mankind is challenged to develop a sustainable, safe and clean means of energy production, which would virtually eliminate the existing dependence on fossil fuels. In this regard, Nuclear Fusion technology would give man a quantum leap to mark a near end to the long-term energy concerns and redefine the basis of energy production on earth and elsewhere. This explanation holds rationale on two principal elements 1-Abundant supply of cheap fusion fuel and 2-Surpassingly superior energy production efficiency.

But, as every boon comes with a 'But', the criticality of technology is that fusion needs inhumanly high and sustainable reaction temperatures. Such temperatures are realized by producing and sustaining Plasma, popularly called the fourth state of matter. Stellarators are a class of magnetic fusion confinement devices used for this purpose. Quasi-Poloidal Stellarator (QPS) is one such device under development at Oak Ridge National Lab. QPS consists of complex shaped modular coils, which are made of Copper-CTD 403 cyanate ester composite to carry the high current needed to develop the Plasma. Due to electrical resistance offered by the coils, tremendous heat is generated, which should be continuously and efficiently removed.

Copper tube embedded coils were identified to provide the best cooling rate through computational analysis [1]. These embedded coils will be hand wound (called lay-up) on a 'form' that takes the final shape of the modular coil within very stringent geometric and magnetic tolerance standards. After lay-up, the conductor is vacuum impregnated with CTD 403 cyanate ester polymer.

The issues pertaining to 'no crimp – lay-up' of the tube embedded conductor have been addressed by having a Low temperature Melting Alloy (LMA) as filler in the tube prior to manufacturing of the conductor. This LMA helps prevent crimps in the tube at sharp bends of

‘race track shapes’ during lay-up and should be flushed out once the lay-up is completed. This retains a clean passage for the flow of cooling water. Problems in filling and flushing the tube with LMA have been investigated experimentally and innovative processes and procedures were developed. Also a complete test modular coil was developed to gain hands on experience in conductor lay-up, impregnation and to understand the cure cycle behavior of CTD 403.

A novel approach was developed to conduct parametric studies on heat transfer in the 200-ft long conductor coil and cooling water with some approximations. A basic model was thus setup and numeric code was developed in MATLAB software. The temperature distribution was compared with finite element models developed in FEMLAB software. The results of this new approach are presented in this work and analyzed to understand the heat transfer at different sections along the conductor over time.

This technique was used to study the effect of several flow and thermal conditions, and geometry and material parameters on the effectiveness of cooling.

TABLE OF CONTENTS

LIST OF TABLES

LIST OF FIGURES

1. BACKGROUND

1.1 WORLD ENERGY FORECAST 2025 AT BRIEF

According to forecasts by Department of Energy – United States in 2004, world energy consumption is projected to grow by 54% by 2025. Fig.1.1 shows the energy consumption forecast in industrialized, developing and Eastern Europe/Former Soviet Union countries. (1 Quadrillion Btu = 1.06 x 10^{15} KJ). World oil consumption would increase from 77 million barrels a day in 2001 to 121 million barrels a day in 2025 with US and developing Asia accounting for nearly 60% of the projected growth in world oil use. World net electricity consumption nearly doubles over the projection period, from 13,290 billion kilowatt-hours in 2001 to 23,072 billion kilowatt-hours in 2025 [2].

Currently of all the coal consumed worldwide, nearly 64% is used exclusively for electricity generation and most countries are trying to reduce their dependence on coal while aiming to go for cleaner and efficient means of power generation. Also reliance on coal and other fossil fuels would substantially increase worldwide carbon dioxide emissions.

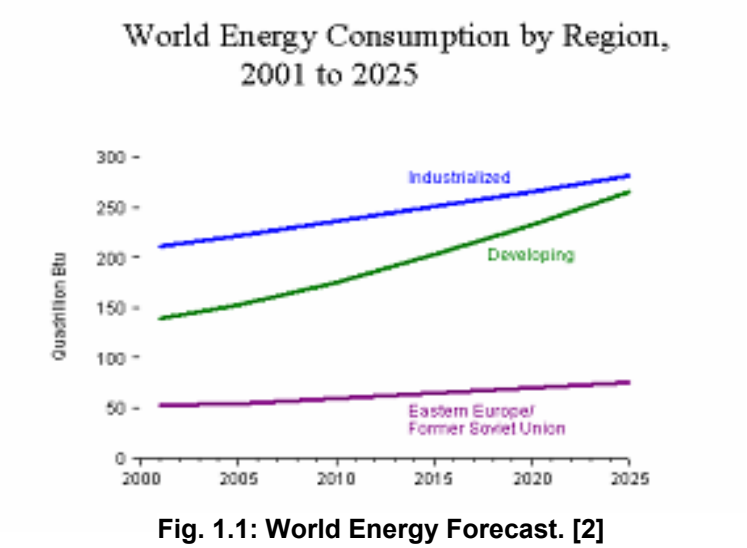

Fig. 1.1: World Energy Forecast. [2]

On the renewable energy front (hydroelectric energy, wind energy etc.) much of growth is expected in wind energy farming across Western Europe and United States. But it is dependent on various factors including geographic conditions and climatic patterns of the farming area, which are not under human control.

On the Nuclear power generation front, production capacity is expected to substantially increase from 2,521 billion kilowatt-hours in 2001 to 3,032 billion kilowatt-hours in 2020, before declining slightly to 2,906 billion kilowatt-hours in 2025 (due to retirements of few plants). Forecasts show there will be 4.1% year on increase in consumption of nuclear power with developing nations accounting for 96% of the projected growth in capacity.

1.2 TYPES OF NUCLEAR REACTORS

Fission reactors – Uses Uranium 235 as fuel (widely used in many countries).
Fusion reactors – Uses Deuterium (obtained from water) and Tritium (obtained from lithium) as fuel (still in R&D).

1.2.1 MAIN ADVANTAGES OF FUSION REACTORS

The fuel needed for fusion reactors is in abundant supply on earth surface and hence cheap and available to all. Output energy is 50-100 times more than energy needed to initiate fusion reaction. The risk of a nuclear accident is virtually nil. There is no air pollution as in using fossil fuels. The radioactive waste is from structural materials activated by the high-energy neutrons. So it is easier to handle unlike the waste from fission reactors. All these advantages improve the economy and safety in power generation.

Therefore, based on the above forecasts it would be efficient, cleaner and ideal to invest capital and increase the nuclear power generation capacity with stringent safety measures, which will ensure zero occurrence of accidents.

The main challenge in fusion reactors is the development, confinement and sustenance of plasma.

1.2.2 DEVICES USED FOR THIS IN FUSION REACTORS ARE OF TWO TYPES

Stellarator eg.: Quasi-Poloidal Stellarator (QPS) (Oak Ridge National Lab), NCSX (Princeton Plasma Physics Lab).

Tokamak eg.: ITER (France), EAST (China), SST-1 (India), KSTAR (Korea).

Stellarators are a class of magnetic fusion confinement devices characterized by three-dimensional magnetic fields and plasma shapes and are one of the best-developed class of magnetic fusion devices. The QPS is a low-aspect ratio, concept exploration experiment with a non-axisymmetric, near poloidally symmetric magnetic configuration. The QPS is currently in the early design phase and is being investigated jointly by ORNL and the University of Tennessee.

QPS uses modular coils of complex shapes often referred to as 'race track shapes' to carry the heavy current required to develop and sustain plasma. A cut-away section of QPS is shown in Fig.1.2. Section of a modular coil is shown in Fig. 1.3. A modular coil consists of tightly arranged pack of conductors. Each conductor consists of continuous copper strands in epoxy matrix (metal matrix composite). The fiber volumetric ratio is approximately 80%. The copper strands were used to provide flexibility to bend the conductor into the complex shapes. The complex shape and orientation of the modular coils provide the necessary electromagnetic field to develop and sustain the plasma when a high current of the order of million amperes is passed through each of the coils. This generates heat in the coils and this heat has to be dissipated. Primary interest of this thesis is to propound different ideas for removing this heat and derive conclusions based on analytical, computational and experimental results.

.

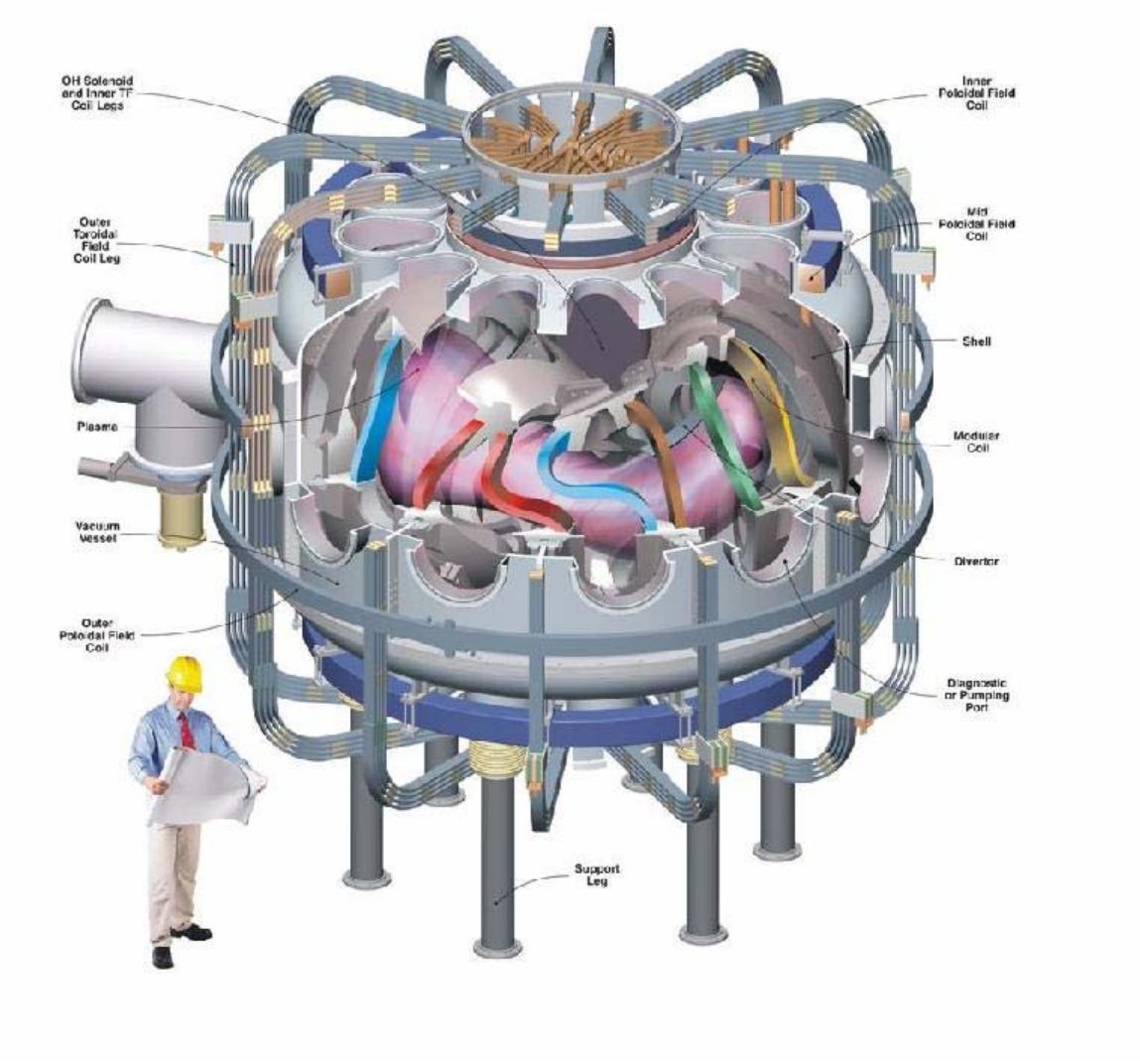

Fig. 1.2: Cut-away section of QPS

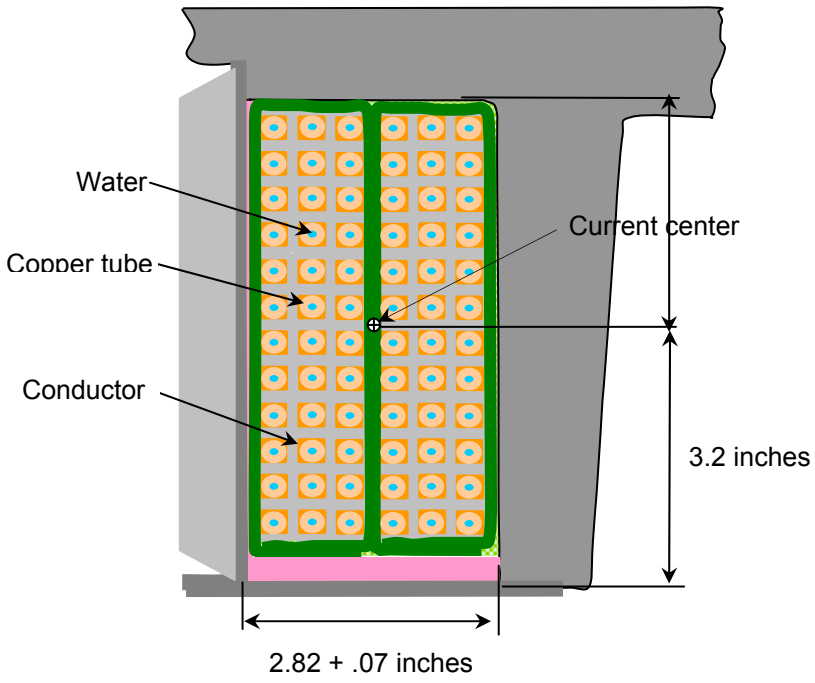

Fig. 1.3: Modular Coil Cross-Section with Internal Cooling Tubes

Various approaches that were analyzed for cooling the modular coils are shown in Fig. 1.4 Freudenberg et al., [1]. It has been concluded that the most efficient method of cooling the coil is the one with copper tube embedded inside every conductor (Option 1 in Fig. 1.4). This provides faster rate of cooling between the current pulses.

Analytical and Computational heat transfer analysis was carried on Option 1 for various flow conditions and results have been presented in this thesis.

The challenges in having an embedded copper tube in the conductor are:

- It is difficult to produce conductors with embedded copper tubes.

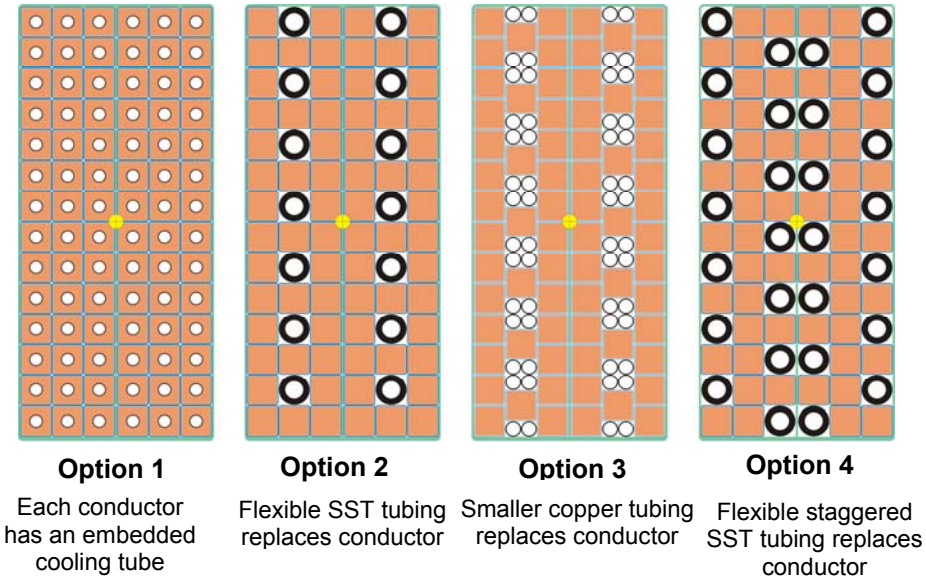

Fig. 1.4: Various cooling concepts analyzed

- During winding and lay up of the modular coil structure these hollow copper tubes have a tendency to kink. Every kink will act as an impediment to the flow of water and the cumulative effect may produce disastrous behavior when not taken care of.
- To minimize kinking/crimping of the soft annealed copper tube during lay-up, it could be filled with a Low Melting Alloy (LMA), which can be melted away once lay-up of the modular coil is completed. This way kinking can be prevented.
- Getting a perfect fill of LMA in 200 feet long copper tube of 3/16-inch outer diameter without trapped air pockets difficult and time consuming.
- Removal of the LMA after the tube laid into its desired complex shapes is again difficult and time consuming. Even a small amount of LMA remaining in the tube can impede the water flow and thus affect the cooling efficiency.
- An embedded tube in the conductor poses difficulty in winding and lay-up of the modular coil. This is because of the strain hardening property of copper. 'Keystoning' has also been of concern with the conductors having embedded tube.

- There has also been a recent surge in copper prices (prices tripled in the 3rd quarter FY06 to nearly $3.9/lb - COMEX prices).

To obviate the above mentioned problems alternate tube sizes, different tube and LMA materials, innovative procedures in filling, and draining the LMA with minimum residual levels were studied for suitability under given constraints of the problem. From further research it was found that LMA could be used but unnecessary for QPS. It also keeps the tube round in cases of high compaction.

2. LITERATURE REVIEW

Many researchers have investigated the effect on heat transfer due to different types of flow of fluids and gases and parameters that affect the heat transfer rate. Studies on heat transfer have been conducted using a) multitude of tubes such as horizontal tube with various cross sections and orientations, b) tubes rotating around a parallel axis as used for internal cooling in some electrical machines; c) cooling tubes with different configurations like straight and wavy tubes (waviness along the length of the tube); slabs etc.

Some of the work pertinent to this thesis has been presented in the following pages.

C.W. Leung and S. D. Probert [3] studied the forced convective heat transfer properties in a duct with triangular cross section. Through an experimental setup they obtained the values of Nusselt number for a range of Reynold's numbers covering the laminar and turbulent phases taking into account the hydraulic diameter.

C.W. Leung and S. D. Probert [4] also conducted the above study for isosceles cross section of the tube. It was concluded in the study that the maximum heat transfer coefficient could be obtained by having the equilateral triangle cross-section for the same hydraulic diameter. Also higher turbulence and rounding of the corners diminished the inhibition to heat transfer posed by the triangular corners.

G. Wang and S. P. Vanka [5] studied numerically the rates of heat transfer for flow through wavy (sinusoidally curved) passages. Beyond Reynold's number of 180, oscillations in the flow led to the destabilization of the thermal boundary layer. During the transitional flow, the heat and mass transfer increased to nearly 2.5 times.

Yasuo Mori et al., [6] investigated the forced convective heat transfer property in a straight tube rotating along a parallel axis taking into account the secondary flow due to rotation about the axis. X. Lu et al., [7] work involved solving a transient multi dimensional heat conduction problem in a composite circular cylinder. Time dependant temperature boundary condition was considered as a Fourier series. A novel approach of applying separation of variables in their multi dimensional case has been presented. This led to almost the same number of calculations as in a one-dimensional case.

X. Lu et al., [8] developed another approach to solve the time dependant multi dimensional composite cylinder slab conduction problem with a time dependant boundary condition. They removed the instability due to the existence of imaginary eigenvalues in other numerical schemes by their approach of using Laplace transforms and separation of variables.

E.K. Kalinin et al., [9] investigated the effects of unsteady convective heat transfer in tubes carrying gases and liquids. The flow was turbulent and the effect of variable flow on heat transfer was studied. The theoretical results were compared with experimental results.

Yuzhi Sun et al., [10] developed a method to solve a transient heat conduction problem in a one-dimensional three-layered composite slab. Eigen function method was used to derive the solution. This method was found to reduce the inaccuracies caused by numerical solutions for the same problem especially when one of the slabs has radically different properties or is much narrower than the others.

F. de Monte [11] developed an analytic approach which is described to be simpler than the earlier models to solve one dimensional transient conduction problem in a multi layered composite slab. The method analyses the heat distribution when the surrounding fluid temperature undergoes a sudden change. Also an example has been shown in the numerical form.

Abram Dorfman [12] investigated the temperature distribution when a thin film of cold fluid is flowing on a semi-infinite flat plate. Evaporation and sputtering were taken into account.

Table 2.1 provides a summary of the above-mentioned research.

Table 2.1: Summary of the published research

Authors	Study conducted	Observations/Conclusions
C.W. Leung and S. D. Probert	• Internal forced convective heat transfer. • Tube: Triangular cross section (equilateral). • Medium: Air.	• Nusselt number in Laminar region is little more than a previous study conducted. • Convective heat transfer coefficient is less than a circular pipe with same hydraulic diameter.
C.W. Leung and S. D. Probert	• Internal forced convective heat transfer. • Tube: Triangular cross section (isosceles). • Medium: Air.	• Convective heat transfer coefficient is less for any isosceles cross section unless all the included angles are 60°. • Increasing the turbulence diminishes the inhibition posed by the corners.

Table 2.1 Continued:

Authors	Study conducted	Observations/Conclusions
G. Wang and S. P. Vanka	• Internal forced convective heat transfer. • Wavy passage (sinusoidally curved).	• Wavy passages improve the heat transfer only when flow is unsteady.
Yauo Mori and Wataru Nakayama	• Internal forced convective heat transfer. • Straight tube rotating along a parallel axis. • Centrifugal force on the fluid.	• Nusselt number ratio is obtained as a function of Prandtl, Rayleigh and Reynold's numbers.
X. Lu, P. Tervola and M. Viljanen	• Transient conduction problem in a multidimensional composite cylinder. • Time dependant temperature boundary condition.	• A novel method is developed to solve their problem. • Earlier analytical approach for solving the heat conduction of composite slab in Cartesian coordinates has been extended using separation of variables for their problem.

Table 2.1 Continued:

Authors	Study conducted	Observations/Conclusions
X. Lu, P. Tervola and M. Viljanen	• Transient heat conduction in multidimensional composite cylinder slab. • Time dependant boundary condition.	• A novel application of Laplace transforms, method of separation of variables and variable transformation obviates the need for residue calculations.
E.K. Kalinin and G.A. Dreitser	• Transient convective heat transfer in a tube. • Turbulent flow of gases/fluids.	• Experiments show the change in flow turbulence has an effect on unsteady heat transfer. • The change in unsteady heat transfer coefficient from quasi-stationary one is not dependent on the variation of boundary conditions themselves but is dependent on the derivative of the variation in conditions like flow rate, wall temperature and flux density. • Heat transfer coefficients were calculated.

Table 2.1 Continued:

Authors	Study conducted	Observations/Conclusions
Yuzhi Sun and Indrek S. Wichman	• One-dimensional transient heat conduction problem. • 3 layered composite slab.	• The advantage of the developed method appears to be eminent when one of the three layers in the composite slab has substantially different thermo physical properties from the other two or when one of the slabs is much narrower.
F. de Monte	• One-dimensional transient heat conduction problem. • Multi layered composite slabs. • Sudden temperature change in the surrounding fluid medium.	• An analytic approach was developed. • Heat exchanged between the composite slab and the fluid was determined.
Abram Dorfman	• Transient convective heat transfer over a semi infinite flat plate	• Investigation on finite wet portion of the plate and dry portion were carried separately.

3. MATERIALS AND METHODS

3.1 OVERVIEW

Based on computational analysis performed on QPS coils by Freudenberg et al. [1], the cooling response between the current pulses is best achieved by providing internal cooling i.e., by having a copper tube embedded in the middle of each conductor. This embedding is done during manufacturing of the conductor. But with this highly efficient cooling some major issues like: 1) crimping of the copper tube during the conductor manufacture (the copper tubes are embedded in the middle of stranded copper conductor by pulling the conductor and the copper tube through a die under high lateral pressure); 2) Crimping of the copper tube during lay-up; and 3) Strain hardening of copper (which poses difficulty during lay-up at tight bends) need to be carefully addressed.

The dimensions of the above mentioned materials used in QPS are: (Fig. 3.1)

Conductor:

Side – 0.393 inches; square cross section; conductor comes wound on spool.

Conductor is wrapped with Glass fiber cloth insulation through its entire length.

Copper tube (Soft annealed):

Outside diameter – 3/16 inch.

Inside diameter – 0.1275 inch and Length – 200ft (approximately)

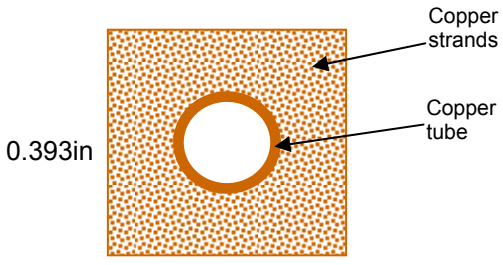

Fig. 3.1: Cross section of a conductor with tube

One of the solutions investigated in this research to prevent crimping of copper tubes is to fill the tube with a low melting point alloy (LMA), such as Bismuth, Lead, Tin and Cadmium in variable amounts. Their melting points range from 70^{o}C – 150^{o}C. The copper tube is filled with an LMA before manufacturing the conductor.

Intended uses of LMA filled copper tube are:

1. Provide crimp protection during the conductor manufacture, and
2. Provides crimp protection during lay-up of the conductor especially at tight bends.

The LMA can be removed during the vacuum pressure impregnation (VPI) of the copper/polymer cure cycle. The melting temperature of LMA is below the maximum cure temperature of the polymer used.

In this study, the following four different types of LMAs (referred by trade names) were used.

1. Cerrotru (Cerro-Bismuth Alloy; 58% Bismuth, 42% Lead; Melting point – 281^{o}F (138.3^{o}C); $39 per 1.5 lbs).
2. Cerrobase (Cerro-Bismuth Alloy; 55.5% Bismuth, 44.5% Lead; Melting point - 255^{o}F (124^{o}C); $25 per 1.5 lbs).
3. MCP124 (Composition undisclosed by MCP; Melting point – 255^{o}F (124^{o}C)) and
4. Cerrobend (Cerro-Bismuth Alloy; 50% Bismuth, 26.7% Lead, 13.3% Tin, 10% Cadmium; Melting point - 158^{o}F or 70^{o}C; $30 per 1.5 lbs).

These four different types of LMAs were investigated to find out the most suitable one for the QPS because they had some distinct mechanical properties like stiffness (high stiffness causes difficulty during lay-up) and physical properties like Melting point and ease of handling, reuse, reaction with water and cost.

The method of filling and flushing the LMA is explained below. For experimental purposes, tube lengths used were 25, 50, 100 and 200 ft.

3.2 FILLING OF THE TUBES WITH LMA

The full length of new soft annealed copper tube (henceforth referred as 'as received') is hand wound on a specially made spool (made from steel sheet) of 14-inch diameter (Fig. 3.2). Care should be exercised while handling the tube for it work hardens quickly. During winding on the spool the C-clamps were used to hold the ends on the tube in place and prevent it from unwinding and slipping off the spool.

After winding the tube, the spool was removed from the mount and placed inside an oven in vertical position so as to use the gravity to fill the tube. Note that Figure 3.2 shows the spool in horizontal position. A funnel was fitted to the top end of the tube, which was sealed to the tube without leaks using fine high temperature cement/paste. Fig. 3.3 shows the complete set-up

Fig. 3.2: 200-ft Virgin tube wound on spool with C-clamps

Fig. 3.3: Spool with tube placed in the Oven (Notice funnel at top end)

placed inside the oven and ready to be heated. The lower end of the tube was raised little higher than the last turn by a few turns to ensure a complete fill in the tube when the molten metal is pouring out at the other end.

The LMA ingots were added in the funnel and the entire setup is heated to a few degrees above the melting point of the metal but always less than 160°C (maximum temperature limitation for flushing the LMA during curing). Cooking is monitored regularly and LMA ingots were added regularly to keep the funnel always filled with the molten LMA and prevent the air entrapment in tube. Sites of air pockets in the filled tube are considered as potential spots where tube crimping may occur. Ingots were added in the funnel until a good flow of molten metal was noticed at the lower end. The lower end was raised to stop the flow and the spool with wound tube was removed from the oven and quenched in ice-cold water immediately. Quenching was done to improve the softness of the tube [13, 14]. Weight measurements were taken for the 'as received' tube and the filled tube and amount of LMA in the tube was calculated.

To understand the extent to which cold water quenching helped, 3 kinds of specimens namely: – 1) Oven cooled; 2) Air cooled; and 3) Quenched in ice-cold water, were prepared and their Load-Deflection behavior was studied using a 3-point bend test setup, Fig 3.4 The results show that the quenched specimens had slightly better stiffness (low stiffness). Based on this, quenching was continued for all the fills.

3.3 FLUSHING OF LMA FROM THE COPPER TUBES

Flushing of the filled tube was performed to test the repeatability and dependability on the process. The spool was placed back in the oven. The oven heated to about 10^{o}C above the melting temperature of the LMA when the liquid LMA started to flow out from the lower end of the tube. Pressurized room temperature air was used from the top end of the tube to push the molten LMA out of the tube.

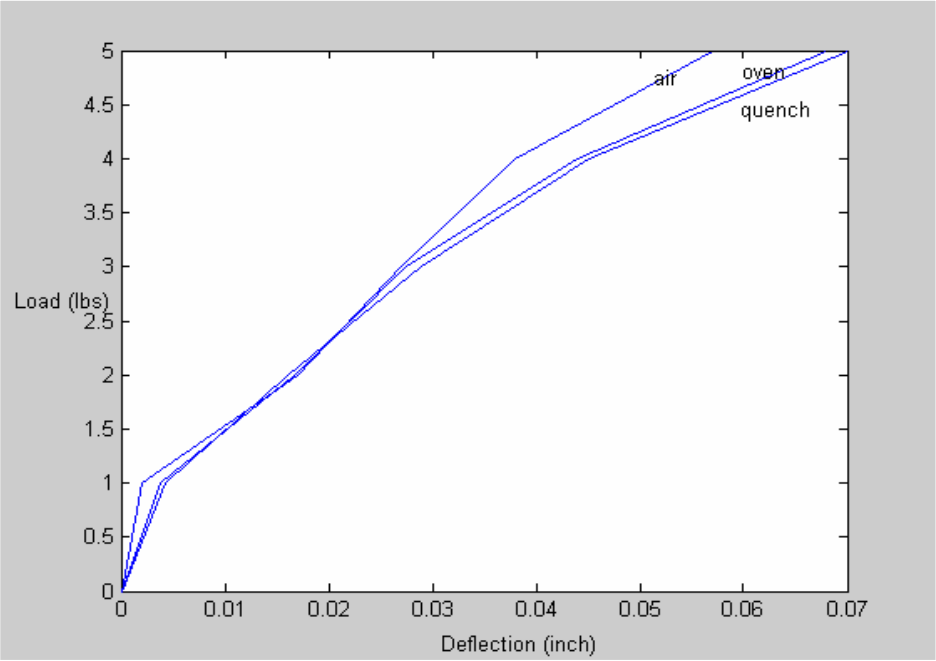

Fig. 3.4: Load-Deflection for differently cooled specimens. The ice-quenched specimen yields the lowest stiffness.

Note that for the most efficient metal removal, hot air should have been used, but our laboratory was not equipped to provide the hot air. The molten LMA was collected and weighed. The tube was then removed from the spool and weighed. This was compared with the 'as received' tube weight and amount of LMA still inside the tube was determined.

3.4 FLOW MEASUREMENTS

Flow measurements were carried out on several lengths to find out the change after filling and flushing the metal out of the tube. In order to prevent the formation of air bubbles along the walls of the tube, the tap water was first collected and left in the room for a day to bring the water temperature to the room temperature. The water reservoir was filled with the water (Fig. 3.5) and the water level in the reservoir was always maintained at the same level to keep the water head the same. The water was collected at the other end of the tube for a given time (for about 5 minutes). Typical results are shown in Tables 3.1 and 3.2.

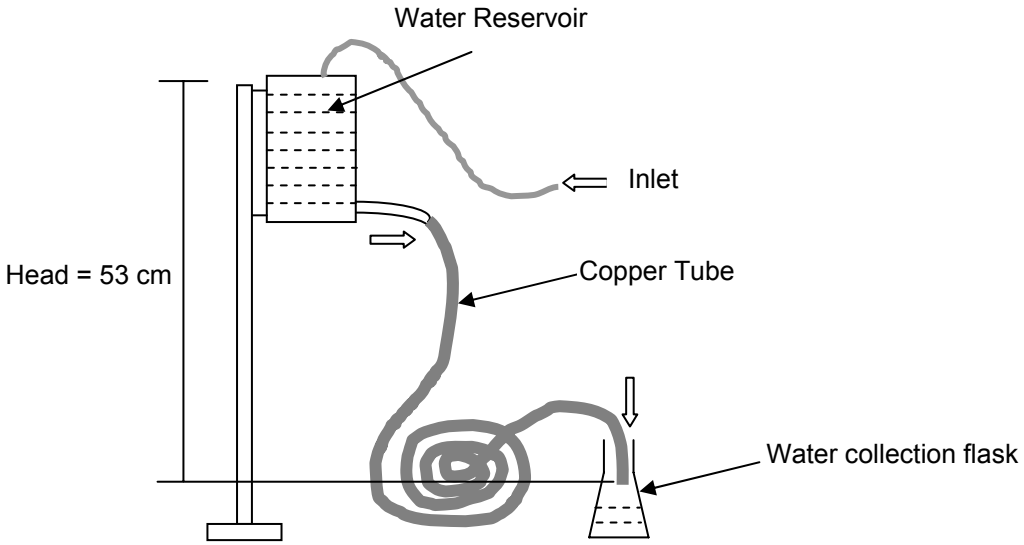

Fig. 3.5: Flow rate measurement set-up

Table 3.1: Weight and flow rate of water for 'as received' coiled 50-ft tube

Time (seconds)	Weight of water collected (gm)	Flow rate (gm/s)
300.22	294.3	0.9803
300.15	293.4	0.9775

Average flow rate = 0.9789 g/s

Table 3.2: Weight and flow rate of water for flushed coiled 50-ft tube

Time (seconds)	Weight of water collected (gm)	Flow rate (gm/s)
300.38	239.5	0.7973
300.31	240.1	0.7995

Average flow rate = 0.7984 g/s

Table 3.3: Weight measurements of coiled 50-ft tube

Empty weight of Copper tube (50-ft long) (gm)	Weight of tube after flushing the LMA (gm)	Weight of LMA removed (gm)
1303.6	1396.8	1193.2
1300.7	1390.8	1191.1

Percentage loss in flow rate = 18.44 % from Tables 3.1 and 3.2.

Table 3.3 shows typical weight measurements of empty and flushed 50-ft copper tube. Weight calculations revealed 7.2 % by weight of LMA remaining in the tube after flushing.

From the above numerical values it was concluded that the cold air at room temperature might have frozen the liquid LMA during flushing. Samples from these tubes were taken at critical bends and they were cut along the length to reveal the inner walls. Examination of the inner wall revealed that there was a thin coating (flakes) of the LMA over the walls in some regions [15].

3.5 ALTERNATE MATERIAL

Due to strain-hardening concerns of the copper tube and some metal sticking to copper tube walls, Teflon tubes seemed another alternative to this problem because of their high flexibility and relatively non-sticky nature [16]. But the thermal conductivity of Teflon is much lower than copper. Because of this the tubes used were of relatively thinner walls to increase the cooling efficiency. The procedure for filling the Teflon tubes with the LMA and flushing the LMA out was same as that used with the copper tubes. Two sizes of tubes were experimented and their advantages and disadvantages are mentioned below:

Size 1: TFT-200-9 (Electrospec)

Inner Diameter – 3.38mm

Wall thickness – 0.38mm

Advantages – Easier to fill, easier to bend, very little spring back observed.

Disadvantages – LMA cracks at sharp bends and the tube is prone to crimp at those places. This small tube diameter will make it difficult to retrofit with metal fittings and the smaller diameter meant smaller flow rates.

Size 2: TFT-250-2 (Electrospec)

Inner diameter – 6.68mm

Wall thickness – 0.5mm

Advantages – Easier to fill, easier to bend, very little spring back and easier to have retrofits.

Disadvantages – Heavy LMA produced sagging of the tube, which made filing very difficult. This would occupy more volume inside the 0.393-inch square conductor.

After weighing the pros and cons of Teflon tubing and from lessons learned, Teflon was rejected for an alternative material and copper was reconsidered.

3.6 PROCESS IMPROVEMENT

Because the numerical values of weight of the material still remaining after flushing process were not encouraging, the process needed improvement. Pre-coating the 'as received' tube with high temperature motor oil (SAE 0W30, Castrol Syntec) was expected to reduce the LMA deposition and it was carried out. Because the flow tests were performed on 'as received' tube prior to filling, there was some moisture in the tube. This moisture reacted with the LMA and motor oil at high temperature and the weight of LMA remaining in the tube raised to 8.7% by weight in 50-ft long tube. To test the chemical reactivity of the cerro alloy (cerro base) with motor oil, both were heated in a beaker up 200^{o}C. Noticeable amount of sludge was formed. Because of this, highly non-reactive, inert high temperature Silicone oil was considered as a replacement of the motor oil. Pre-coating did prove helpful to a great extent. The results showed a considerable improvement in removing most of the LMA leaving only 0.15% by weight in the tube. To study the nature of the mass left behind, the tube was cut along the length and the sections were

examined. The little LMA left behind was in the form of small pellets and flakes of low density but with more volume than expected. The presence of pellets was considered unacceptable because these pellets could lodge themselves in tight bends and greatly impede the water flow during the actual operation.

Altering the set-up while still maintaining the basic methods further improved this process. In this improved set-up (Fig. 3.6), pressurized hot water was used to flush the LMA (Cerro bend was selected for this experiment because of its low melting temperature of 70^{o}C) out of a 200-ft long filled tube. Water was heated to just below its boiling point in the 1st oven and the filled tube in the 2nd oven. Air was pressurized at 20 psi and this pushed the hot water through the tube. LMA was flushed in 15-20 seconds. Just to ensure a clean flush, the pressure was increased up to 90 psi to create turbulence and flow direction was reversed in the tube for 20 seconds. Some of the molten LMA still remaining gushed out and then a stream of hot water followed. The weight and flow rate measurement results are shown in Table 3.4.

The slight increase in flow rate after flushing was attributed to the increase in the volume of cerrobend as it solidified [17]. It was determined that 50^{o}F is the ideal quench temperature [18]. From the above values it was concluded that flushing was successful with pressurized hot water. Now with this improved set-up, vacuum pump was attached and used for clean filling of the

Table 3.4: Comparison by weight and flow rate of 'as received' and flushed Copper tube

Description	As received	After flushing
Weight of 200-ft Copper tube	5412.8 gm	5410 gm (2.8 gm less than original)
Flow rate of water	0.31 gm/s	0.33 gm/s (slight increase in flow rate)

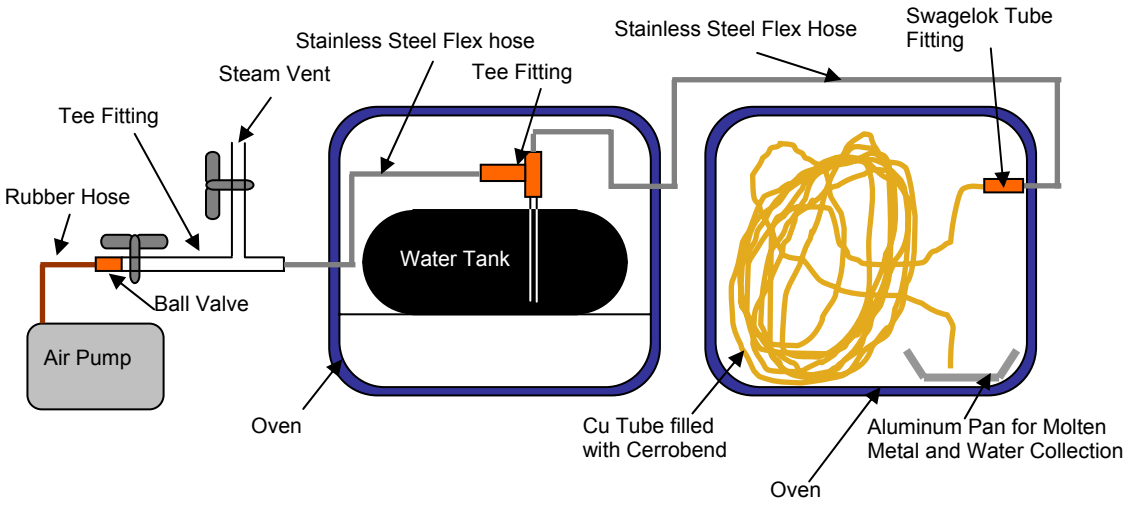

Fig. 3.6: Improved set-up for flushing

'as received' tube. Pre-coating with Silicone oil was still performed. A complete description of filling the copper tube with this improved setup is given below:

Fig. 3.7 shows the new setup used for filling. To start with, inspect the inside of the two Stabil Therm Ovens for cleanliness. Clean the oven as necessary. Place a 2-1/2 gallon paint tank in oven "A". The tank will act as a vacuum reservoir. Remove the lid of the paint pot and secure. There will be two connections at the top of the paint tank. Connect one of the connections to the vacuum pump and the other to a flexible hose (inside an insulated pipe), which will extend from oven "A" to oven "B". There will be a sight tube (clear) connected to the flexible hose inside oven "A" and interface with the second connection from the top of the paint tank. Place one spool of 3/16" copper tube in oven "B". Place a 3-1/4 qt. stainless steel beaker within the inside diameter of the coiled tubing.

The lower most end of the coiled tubing will be the lead or supply and the upper most end of the tubing will be the tail. Extend the lead end of the copper tube upward toward the inside roof of the

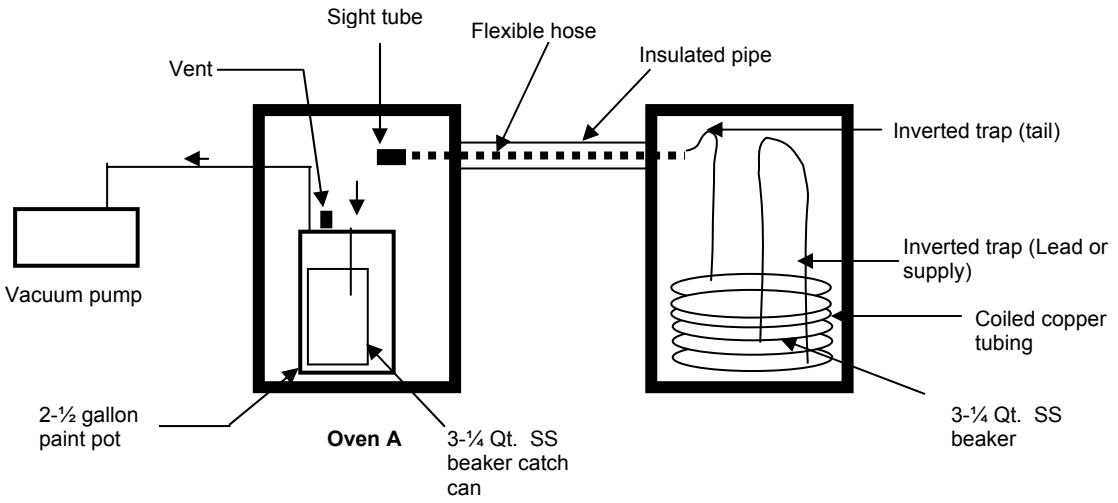

Fig. 3.7: Improved set-up for filling

oven and back to the bottom of the stainless steel beaker. This will form inverted lead or, supply trap. Take the tail end of the coil and extend it upward toward the inside roof of the oven and create a loop downward toward the flexible hose and connect. This will create an inverted trap at the tail end of the copper tube to prevent siphoning of the fill material. The two traps in oven "B" are essential and from a "holding boundary" of material, which must be held in the inside diameter of the coiled tubing when vacuum is turned off and the tubing vented to atmosphere. Pour one qt of silicon oil in 3-1/4 qt stainless steel beaker in oven "B". Verify all connections are tight and the lead or supply end of the copper coiled tubing is in the base of the stainless steel beaker filled with silicon oil.

After the setup is complete, turn on each oven and set temperature at 90ºC. Once temperature has been stabilized and silicone oil heated, turn on vacuum pump and open valve to create a vacuum. Continue pumping until silicone oil is observed in the sight tube. Once silicone oil is observed in sight tube, turn off vacuum pump and vent to atmosphere. The silicone oil will remain in the coiled copper tubing between inverted traps.

To help facilitate the introduction of melted cerrobend, on a separate heating plate, place 9 cerrobend ingots in a stainless steel beaker. Each ingot weighs about 650 gm. Cover the ingots with silicone oil to assure that the melted cerrobend is NOT exposed to atmosphere [14]. Place the ingot filled beaker into another beaker filled with water. The two beakers shall be separated with an insulator block, such as G-10, or similar material. This will create a “double boiler”. Apply heat to the double boiler until the melting of the ingots occurs. Observe the surface of the melted cerrobend. A “dross” will form and must be scraped off, using a stainless steel strap, before impregnating the inside diameter of the copper tubing.

Once the cerrobend ingots have been melted and dross removed from the surface, remove the stainless steel beaker with silicone oil from oven “B”. Place the stainless steel beaker with the melted cerrobend in oven “B” within the inside diameter of the coiled copper tubing. Place the

lead, or supply, end of the copper tube into the melted cerrobend. Assure that the end is at the bottom of the beaker with the same configuration as used with the silicone oil. Close oven door and allow temperature to stabilize at 90ºC. Turn on vacuum pump and open the valve to the paint tank. Observe the flow of the remaining silicone oil in the tubing as the melted cerrobend is being drawn into the tubing. Continue observing the flow of material through the sight tube. Once cerrobend is observed in the sight tube turn off the vacuum pump and vent the paint tank to atmosphere. Disconnect the tail and lead ends of the copper tubing and remove and coiled tubing from the oven using hot gloves. Place the heated copper tubing with cerrobend in to a pool of water to quench the cerrobend.

Experiments were performed using 200-ft length copper tubes and Cerro bend as LMA. The process produced excellent results.

The strain hardening during lay-up as mentioned in 3.1 was not addressed because copper anneals at approximately 500°C, which is much higher than the LMA melting temperature.

3.7 BEND TESTS ON CTD 403

Three-point bending was performed on CTD 403 epoxy specimens to study the stiffness properties of the resin. CTD 403 is used as a resin for the copper conductor. To check the correctness and accuracy of the 3-point bending set-up, a known aluminum alloy was tested. The deflection readings were recorded using a strain gauge and amplifier set-up. The details of the strain gage used for the experiment are:

Resistance – 350 ohm and Gage factor – 2.13; Precision strain gages; Manufacturer – Micro-Measurements Division, Measurements Group, Inc.

An expected result of 67.9 GPa was obtained for the aluminum alloy and through this, the strain gage/amplifier set-up and processes were validated. Three specimens of CTD 403 were tested and the modulus values obtained were 4.74 GPa, 4.45 GPa and 4.16 GPa respectively. Fig. 3.8 shows the actual values obtained for median specimen 2 (4.45 GPa; Dimensions: width = 7.49 mm, height = 5.98 mm, total length = 200 mm).

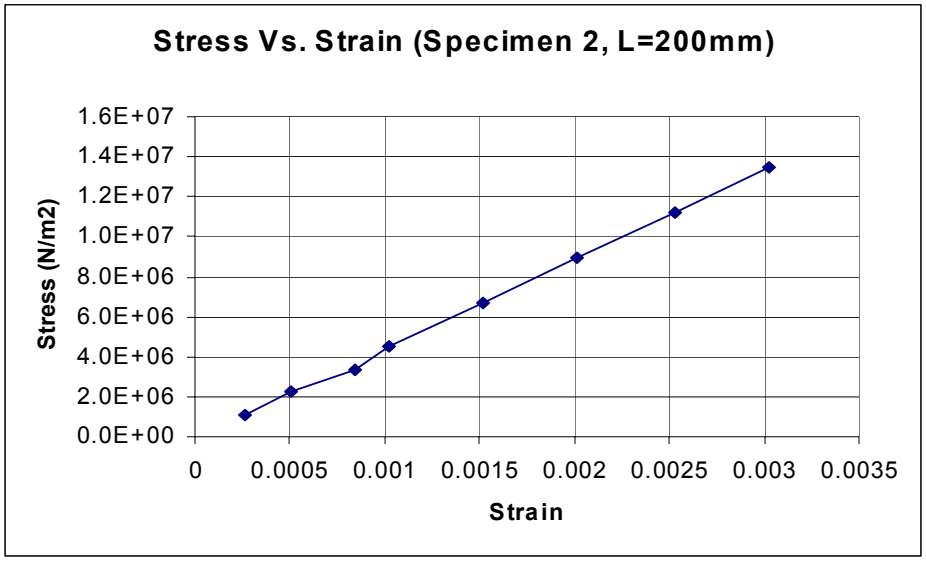

Fig. 3.8: Specimen 2 (CTD 403), Stress - Strain plot

3.8 VACUUM PRESSURE IMPREGNATION

To get an experience and evaluate the feasibility/difficulty in the lay-up process and in handling CTD 403 through the entire curing process, test lay-up was carried using the copper conductor without the cooling tube. The conductor was wound on a form (that was molded in the shape of the final coil) of 2 conductors in width and 2 conductors in height. Fig. 3.9 shows the conductor wound on the form and ready for vacuum impregnation. Some keystoning was noticed at tight corners. Periodic tapping of the conductor at very short lengths as it was wound on the form reduced keystoning. Test lay-up with 'tube embedded conductor' will be carried out in future.

Curing was carried out according to the cure cycle suggested by the CTD 403 manufacturer (Composite Technology Development, Inc.). The cure cycle used originally was 1) From room temperature to 80ºC with 2 hour ramp 2) Hold at 80ºC for 16 hours 3) Ramp to 150ºC for 3 hours

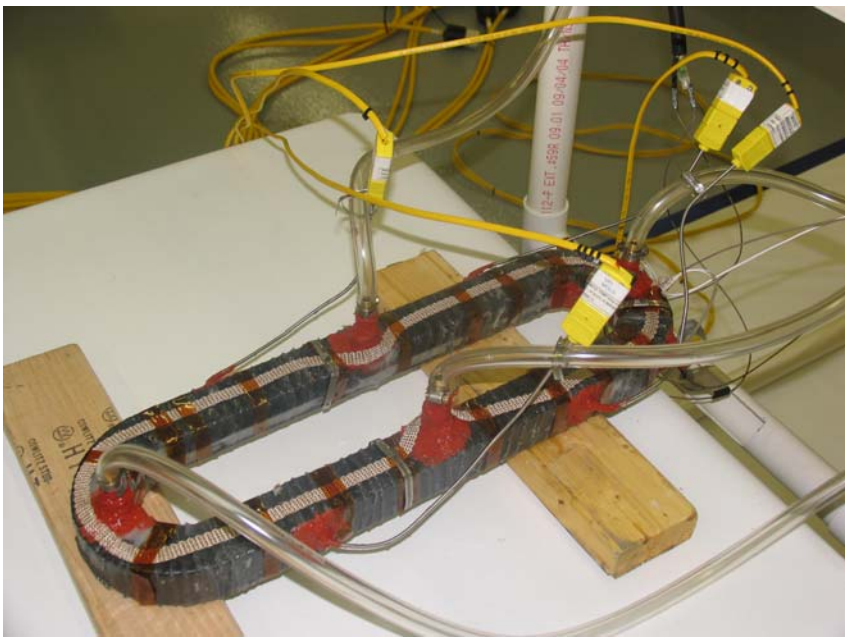

Fig. 3.9: Coil wound on the form. It is sealed with tapes and connected to tubes leading to vacuum pump and is ready for epoxy (CTD 403) impregnation

4) Hold at 150ºC for 4 hours. But this cure cycle was modified to the following after the first test coil. The modified cure cycle is 1) From room temperature to 110ºC with 3 hour ramp 2) Hold at 110ºC for 8 hours 3) Ramp to 150ºC for 2 hours 4) Hold at 150ºC for 4 hours 5) Ramp to 175ºC for 2 hours 6) Hold at 175ºC for 4 hours [19]. The final test coil after curing and removal of insulation tapes is shown in Fig. 3.10. The mechanical testing of this test coil is currently underway at Oak Ridge National Laboratory.

Fig. 3.10: Test coil after curing and cleaning

4. HEAT TRANSFER ANALYSIS OF THE CONDUCTOR

Heat transfer analysis of the conductor was carried out computationally using the finite element analysis and compared with another independently developed model. Temperature distribution in the conductor due to heat carried away by the cooling water flowing through the embedded copper tube was determined as a function of time. Finite element model of the conductor with tube was developed using FEMLAB 3.2 (COMSOL). The conductor used in QPS is a metal matrix composite with Copper strands in CTD 403 cyanate ester in 80:20 volumetric ratio. The initial temperature of the conductor and temperature of inlet water used in the model were 60°C and 20°C, respectively. The material properties of the composite (conductor) and water were used with other known heat transfer boundary conditions. One major limitation in using the finite element software was the limit on the number of elements/nodes allowed by the educational version of the software available for this study, which limited the maximum conductor length to be about one inch, whereas the actual conductor length used in QPS is around 67m (~200 ft).

To overcome the above issue, a novel analytical approach was developed and implemented for the same model of length 1-inch (as in FEMLAB) using MATLAB 7 to compare and validate the correctness of the approach. On finding similarity in trends and numerical values, the analytical approach was extended to higher lengths up to the required maximum length of 200-ft.

4.1 FINITE ELEMENT MODELING THE PROBLEM

A three dimensional model was developed in FEMLAB. Due to symmetry in cross section of the original problem, the model was reduced to a quarter as shown in Fig. 4.1. The dimensions of the model are shown in Fig. 4.2. The thickness of the copper tube was neglected and the water passage was assumed to be a mere hole in the composite as shown below. The length of the model analyzed was 1-inch.

Table 4.1 shows the material properties used for different models analyzed in FEMLAB 3.2.

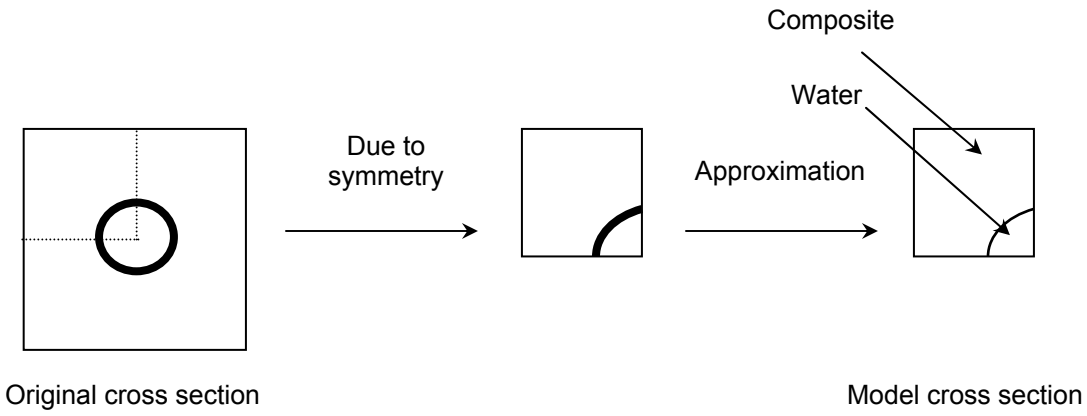

Fig. 4.1: Finite element Model used in FEMLAB

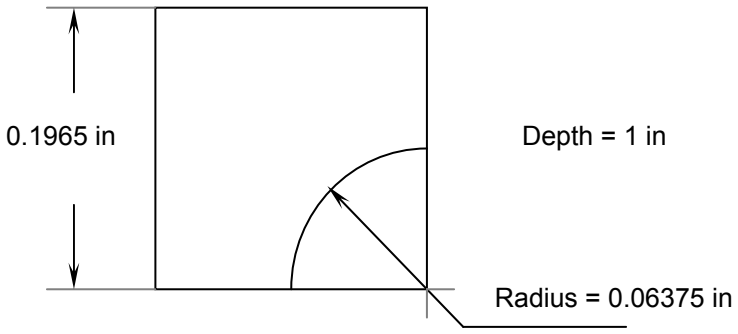

Fig. 4.2: FEMLAB model dimensions

Table 4.1: Properties of composite and water used in the FEMLAB models

Property	Composite	Water
Density (Kg/m^3)	6705	1000
Thermal conductivity (W/(m.K)	12 in the width and breadth directions, 320 along the length (high conductivity is due to continuous copper strands along the length).	0.6
Specific heat (J/(Kg.K))	688	4200
Initial temperature (K)	333	293
Velocity (m/s) (Used for only 3-D models).	-	1, 2, 3 and 4 (4 different models were solved).

The specific heat (Cp) of the composite was calculated from its constituent properties using the 'Rule of mixtures' as follows:

Cp of Composite = 0.8 Cp of Cu + 0.2 Cp of Epoxy

Cp of Epoxy = 1900 J/(Kg K) - Approximated [22]

Cp of Cu = 384 J/(Kg K)

Cp of Composite = 688 J/(Kg K)

Cp of Water = 4200 J/(Kg K)

4.2 ANALYSIS OF A FEMLAB 2–D MODEL

Before the actual model was analyzed, a 2 dimensional model was developed with the same cross sectional dimensions (as in Fig. 4.2) and a transient conduction problem was solved. Insulated boundary condition was applied on all sides thus restricting the heat transfer to only the composite-water interface. This analysis was carried to study the proximity of the finite element results with analytical results.

The analytical steady state temperature was calculated by equating the total heat crossing the composite – water interface as follows:

$$-m_c \times Cp_c \times (T_{ic} - T_f) = m_w \times Cp_w \times (T_{iw} - T_f)$$

where m – mass

Cp – specific heat

T_i - Initial temperature

T_f - Final temperature

Subscripts ‘c’ and ‘w’ represent composite and water respectively. Negative sign on left hand side of the equation represents heat lost by the composite. Based on the above calculation the steady state temperature (T_f) obtained was 56.98°C (134.6°F). The transient conduction problem converged close to this number in nearly 20 seconds and the results were satisfying to proceed with further analysis. The results are shown in Fig. 4.3.

3–D modeling was done using FEMLAB (dimensions as in Fig. 4.2). Table 4.2 shows the mesh details. Fig. 4.4 shows the planar view of the meshed model.

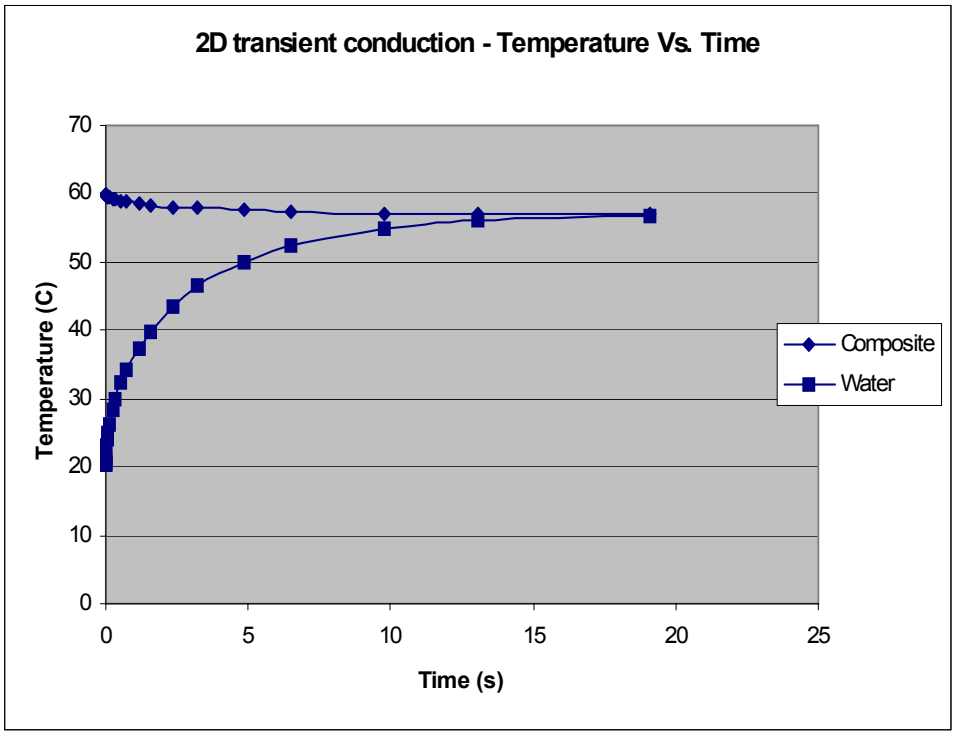

Fig. 4.3: Plot of 2D conduction problem

Table: 4.2: Details of the mesh used in 3D models

Total elements used in the model	48,995 (Quadratic elements)
Degrees of freedom elements	72,446
Number of boundary elements	10,936
Number of edge elements	478
Maximum element size on the composite-water interface surface	0.000254 (with an element growth rate of 1.1 in all directions from this surface) (100 elements along length of the boundary).

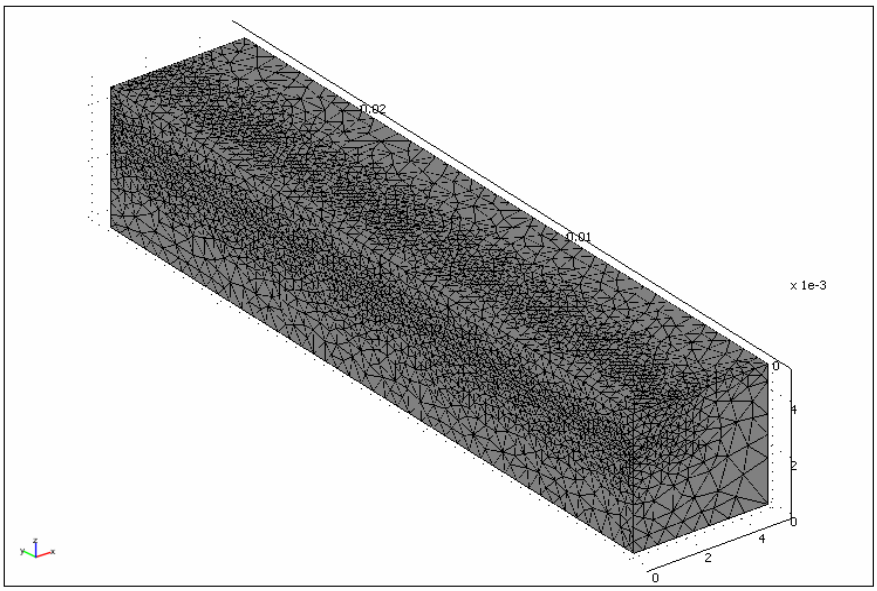

Fig. 4.4: Meshed model

4.3 ANALYSIS OF FEMLAB 3–D MODELS

4.3.1 FLOW DETAILS

The tube was assumed to be filled with water (as an initial condition at time t=0 seconds). A fully developed flow was assumed with a paraboloid profile.

The velocity at any point in water is given by the equation

Velocity = $v_{\max} \times [1 - \left(\frac{r}{R}\right)^2]$

where $v_{\max}$ – maximum velocity of water (tip of the paraboloid)

$r = \sqrt{x^2 + (z - 0.005)^2}$ (where x and z are the coordinate positions along sides of the square cross section of the model as in Fig. 4.5)

R – maximum radius of the water sub domain. (Distance between points A1 to A2 as in Fig. 4.5)

The inlet velocities used for the analysis were 1, 2, 3 and 4 m/s.

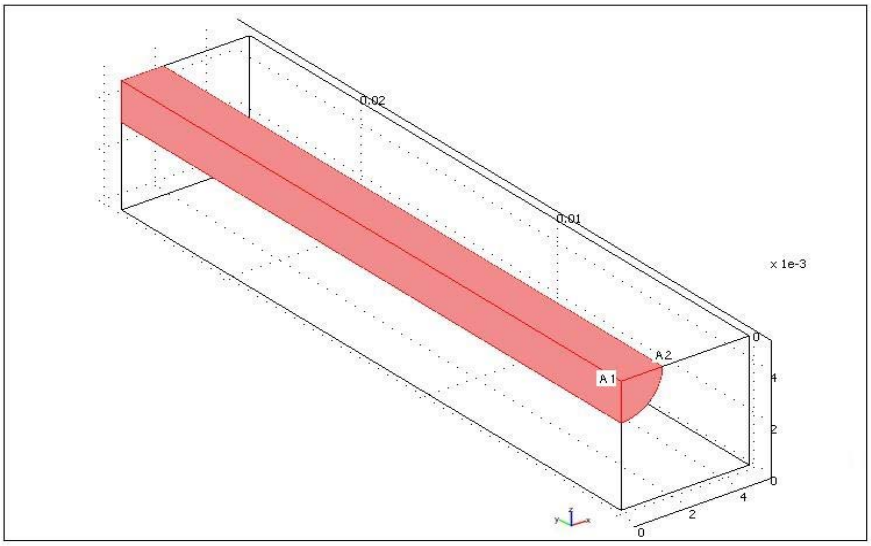

Fig. 4.5: 3-D model used in FEMLAB

4.3.2 HEAT TRANSFER CONDITIONS

Initial conditions:

Water temperature: 293K or 20°C or 68°F

Composite temperature: 333K or 60°C or 140°F

Boundary conditions:

Inlet water temperature: 293K or 20°C or 68°F

Insulated on all outer surfaces and a convective flux boundary condition at the water exit.

This model was solved in 'Heat transfer module → General Heat transfer → Transient analysis' application mode of FEMLAB.

FEMLAB Solver Parameters:

With the above mesh parameters; flow conditions; initial and boundary conditions, a transient analysis was carried out at time steps of 0.01 seconds. Direct (UMFPACK) linear solver was

used. The problem was solved for 'temperature' distribution and results obtained are shown in the next chapter.

Major problems encountered in using a model longer than 1 inch for analysis were:

1. Limitation on the maximum number of elements to be used in the model, which was due to the educational version of the software being used.
2. Limitation on using the computer memory for running the program.

First limitation could have been overcome by reducing the model to ½ its size by considering a plane of symmetry. This way the length of the model could have been increased by few inches. But this could have never been applied for a required length of nearly 67m (~200-ft) with the available resources. So there was an increasing need to use another approach (section 4.4), which could be applied for 200 feet length of the conductor.

4.4 ELEMENTAL APPROACH

In this approach [20], the composite and water are divided into equal number of elements of uniform length as shown in Fig. 4.6. The original approach laid by Mr. Goranson was extended to QPS.

Each water element undergoes heat transfer with each of the composite element as it moves along the tube from inlet to outlet. It is assumed that the water elements stop for a very small time (called time step) for heat transfer with the composite element as it moves towards the outlet.

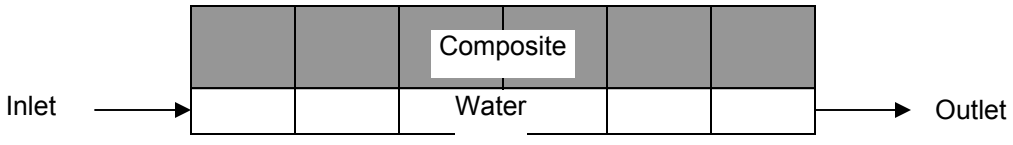

Fig. 4.6: Elemental approach

This continuously happens for all water elements until the prescribed length of cooling time is reached.

To understand how this works, consider the inlet end of the tube. When one water element enters the tube at 20°C (68°F), change in temperature of water element is calculated from heat lost by 1st composite element in one time step (Fig. 4.7). This is the initial temperature of water element in contact with 2nd composite element at next time step. Another water element at 20°C (68°F) enters the tube at the same instant and the 1st composite element is at the lower temperature than the initial. This happens across the tube length for a given length of time.

The temperature of the composite element can be obtained from the following equation [21]:

$$\frac{T - T_2}{T_1 - T_2} = e^{-Bi \times Fo}$$

where T is the final temperature of the composite element after interacting with water (required)

T_1 is the initial temperature of composite (60°C or 140°F at time = 0)

T_2 is the initial temperature of water (20°C or 68°F at time = 0)

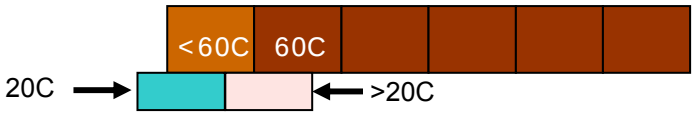

Fig. 4.7: Movement of elements

Bi is the Biot number (*Bi* = $\frac{hL}{k}$ where *h* – convective heat transfer coefficient, *L* – characteristic length, which is volume over heat transfer area, $L = \frac{(r_2^2 - r_1^2)}{2r_1}$, r_2=0.00564 m & r_1=0.00162 m; *L*=0.009 m, *k* – thermal conductivity of composite which is 12 W/m.K. *Bi* is assumed to be 1) and *Fo* is the Fourier modulus ($Fo = \frac{\alpha t}{L^2}$ where α - thermal diffusivity, *t* – time step)

From the above equation, the final temperature *T* of the composite is calculated.

Then heat lost by the composite element and heat gained by the water element are calculated using the conservation of energy as:

$$-m_c \times Cp_c \times (T_{ic} - T_f) = m_w \times Cp_w \times (T_{iw} - T_f)$$

where T_f is the final temperature of water

This water element with the increased temperature moves to the next position and interacts with the 'already' cooled composite element based on the same assumptions.

In this elemental approach only the bulk temperature of the elements are considered unlike in the FEMLAB where a temperature gradient exists along the width of the model. Also the temperature gradients in the elements are neglected and a conduction-only model is assumed. Thus a convection problem is transformed into a conduction problem using Lumped analysis method and the Biot number is assumed to be 1. This means that the resistance to conduction inside the composite element and the resistance to convection are equal. Thus the model becomes a conduction model and the temperatures predicted by this model will give an envelope beyond which cooling is not possible.

In the following chapter, a comparison has been made to understand the effect of change in Biot number on the temperature distribution in the conductor.

The elemental approach was written as a computer code in MATLAB 7 (refer Appendix) and the problem was solved for 67 m (~200 ft) length at prescribed velocities of 1, 2, 3, 4 and 5 m/s.

Analyses on temperature distribution of the conductor for inlet water temperatures of 0°C (32°F) and 10°C (50°F) at 2 m/s were carried out and results were investigated.

5. RESULTS AND DISCUSSION

Investigation on 3-D FEMLAB models and the analytical models with geometry (Fig. 4.2), material property (Table 4.1), initial condition, boundary condition and flow parameter (4.3.1) as mentioned in Chapter 4 was carried for a given length of time. The results are presented and discussed in this section.

5.1 FEMLAB ANALYSIS RESULTS

A full-scale temperature plot of the model solved at inlet water velocity of 2 m/s for 15 seconds is presented in Fig. 5.1. As it can be seen from the figure, the maximum temperature that occurs in the composite is 24.8°C (297.8K) at the end of 15s. The minimum temperature in the water falls to 0.5° below inlet temperature of 20°C(293K). This may be attributed to finite element software error. (The error was higher up to 4° for lesser number of elements in the model. Using higher

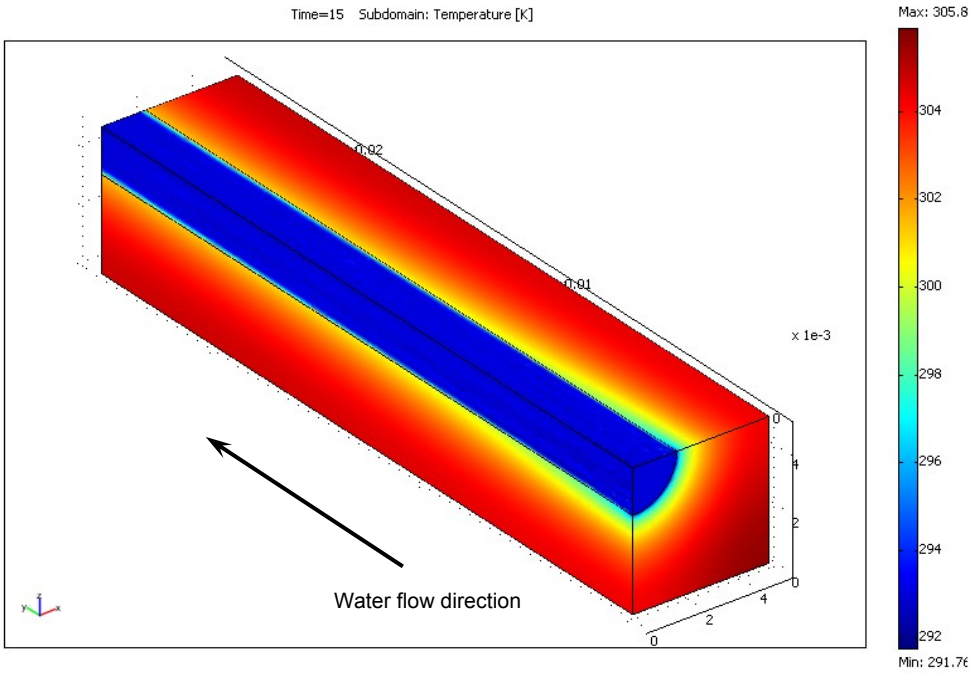

Fig. 5.1: FEMLAB subdomain plot of 1-inch model (v = 2 m/s, t = 15 s)

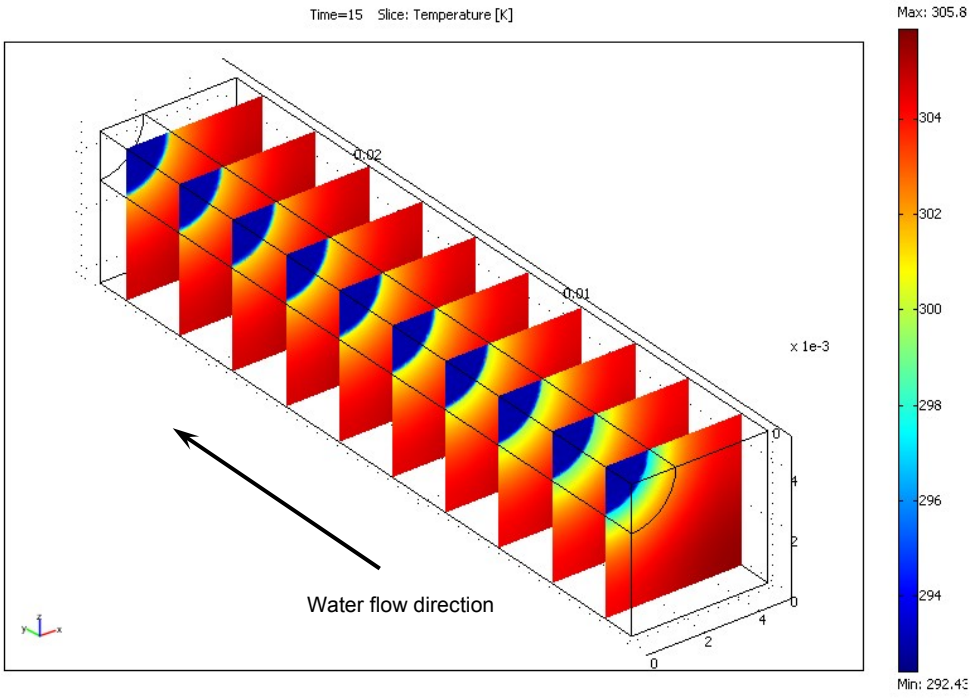

Fig. 5.2: FEMLAB slice plot of 1-inch model (v = 2 m/s, t = 15 s)

number of elements may reduce this error. But due to limitation on the maximum number of elements allowed in the educational version of the software, the number of elements used for all analyzes were 48,995).

A sliced view of the same model is shown in Fig. 5.2. The temperature distribution at each cross section may be noticed as a gradation in color.

Fig. 5.3 shows bulk temperature of conductor and water plotted as a function of time. The bulk temperature is obtained by dividing the 'subdomain (composite) integration for temperature' value from the software by the volume of the composite used in the model. Bulk temperature of water is similarly calculated by dividing the 'subdomain (water) integration for temperature' value by its volume. It can be noticed from Fig. 5.3 that the bulk temperature of water rises to a maximum of 22.9^{o}C at time 0.1 s. It may be noticed that the software initially uses finer time steps for solving.

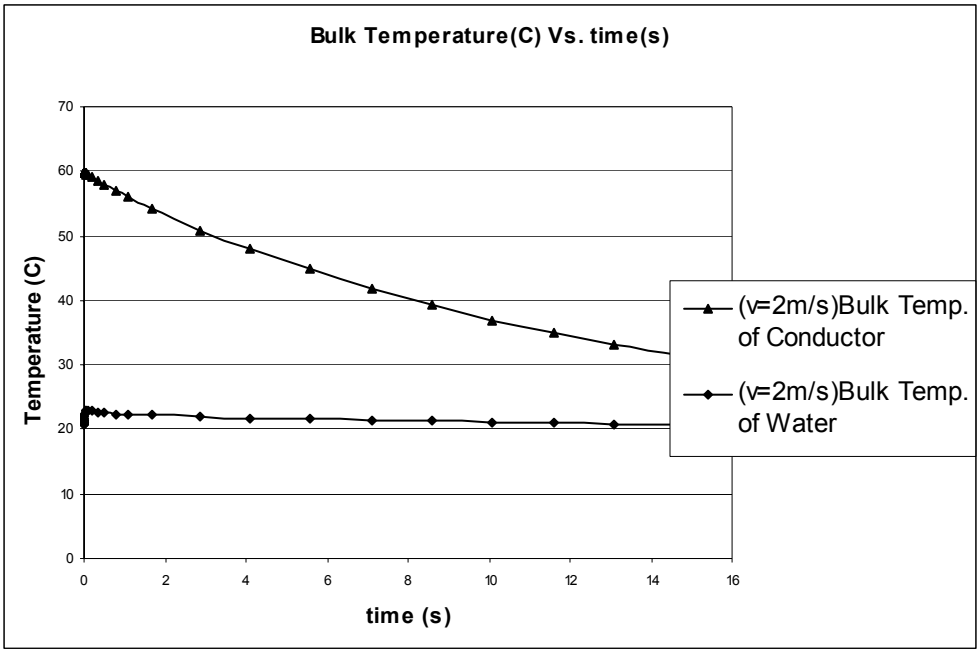

Fig. 5.3: Bulk Temperature Vs. time plot (v = 2 m/s, t = 15s). The initial rise in water bulk temperature is because the tube is filled with cold water at t = 0s. More heat is transferred initially to water from the conductor.

This explains more number of data points when time is small. Reducing the time step increases the accuracy of the solution. But due to computer memory constraints time step used for all analyzes were 0.01s. The initial portion of Fig. 5.3 (from time 0 to 0.5 sec) is replotted in Fig. 5.4. The initial rise and fall in water temperature may be clearly noticed in Fig. 5.4. Because the whole tube is filled with water at 20°C, more heat is transferred initially. This explains the initial rise in water temperature. Similar analysis was carried for different inlet velocities such as 1, 3 and 4 m/s. For all the analysis the inlet water temperature was maintained at 20°C. Fig. 5.5 shows the bulk temperatures of composite and water plotted as a function of time for different velocities. Table 5.1 shows the bulk temperatures at t = 15s and the maximum bulk temperature of water.

The analysis for a velocity of 2 m/s on the 1-inch model was extended to 30 seconds in order to investigate temperature distribution at longer time intervals. Fig. 5.6 shows the Bulk Temperature versus time plot.

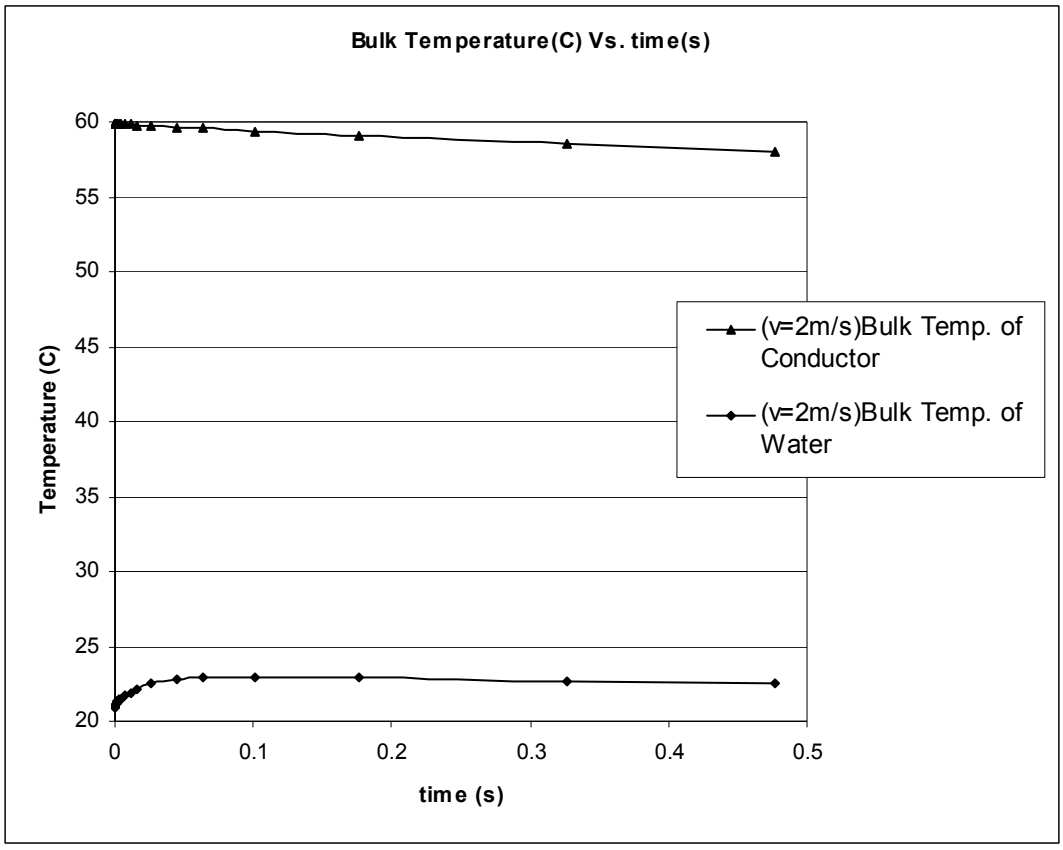

Fig. 5.4: Initial rise in bulk temperature of water. ΔT between water and conductor is maximum when the conductor is hot. It decreases with time and so the bulk temperature of water reduces with time and approaches 20°C as the conductor cools down.

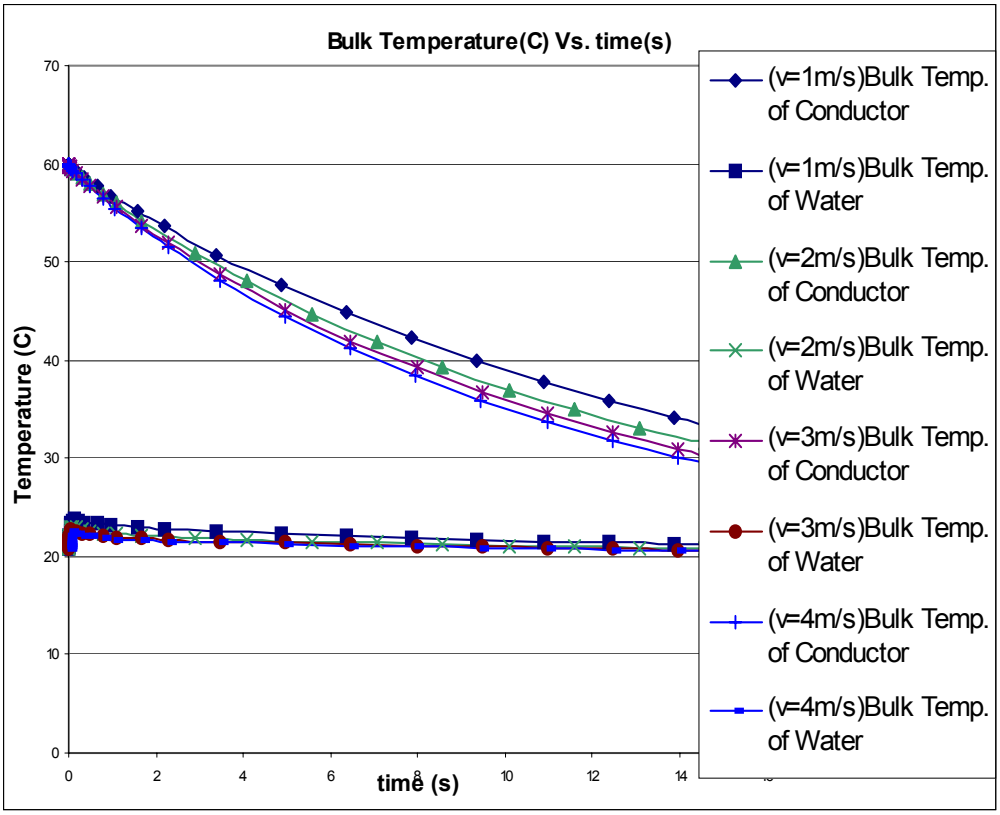

Fig. 5.5: Temperature Vs. time plot for different inlet velocities of water. There is nearly a 5°C between 1 m/s and 4 m/s flow at the end of 15s.

Table 5.1: Temperature specifics of Fig. 5.5

Description	v = 1m/s	v = 2m/s	v = 3m/s	v = 4m/s
Bulk temperature of composite at t=15s	32.98°C	31.11°C	29.95°C	29.13°C
Bulk temperature of water at t=15s	25.16°C	20.79°C	20.63°C	20.59°C
Maximum Bulk temperature of water	23.74°C at t=0.1386s	22.98°C at t=0.10096s	22.67°C at t=0.063122s	22.48°C at t=0.044174s

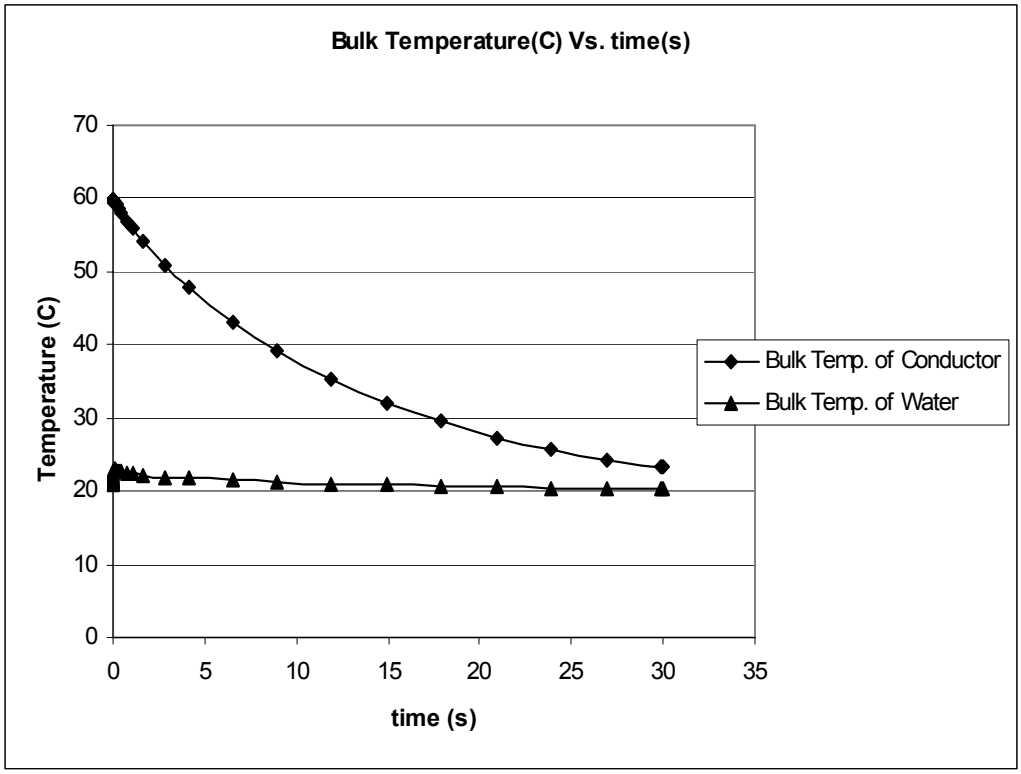

Fig. 5.6: Bulk Temperature Vs. time plot (v = 2 m/s, t = 30s)

In the above plot, the conductor has been cooled to a bulk temperature of 23.29°C by the end of 30 seconds. The water bulk temperature was 20.34°C.

5.2 'ELEMENTAL APPROACH' RESULTS

Water and conductor temperature as obtained from the elemental analysis for 1-inch long conductor is shown in Fig. 5.7. The water velocity used for this analysis was 2 m/s and the length of the conductor was divided into 10 elements (each element of length approximately 2.5 mm). Maximum length of time used for the analysis was 300s. The purpose here was to compare the results with those obtained from the finite element analysis.

The initial portion of water temperature curve (from t = 0 to 1.5 sec) of Fig. 5.7 is replotted in Fig. 5.8. The initial increase in bulk temperature of water followed by the slow decrease is similar to the trend obtained from the finite element analysis of section 5.1. The time scale used for plotting is approximately 1s.

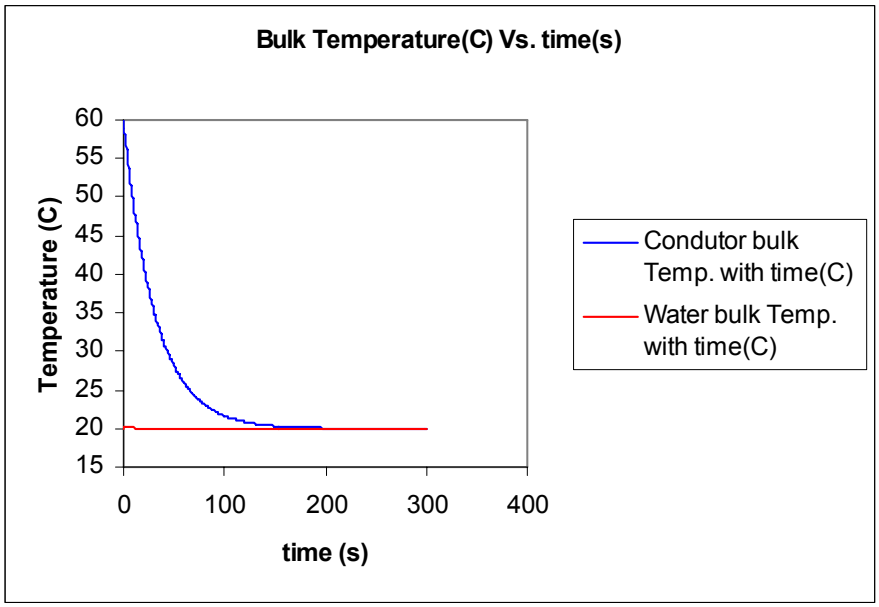

Fig. 5.7: Temperature - time plots for 1-in conductor. Notice a slight early increase in bulk Temperature of water.

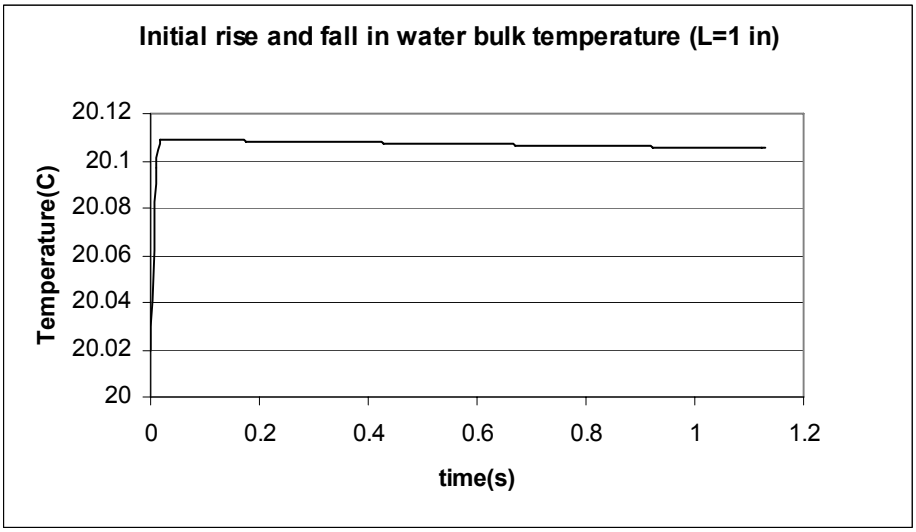

Fig. 5.8: Initial rise in water bulk temperature (L=1 inch)

From the plot shown in Fig. 5.7 it can noticed that the bulk temperature of 1-inch long conductor falls from initial 60^{o}C to nearly 44^{o}C by the end of 15s (In FEMLAB it was 31^{o}C). The difference in numerical value is because of the approximations such as no axial conductivity and assumption of Biot number. In the elemental approach only the bulk temperature of the elements is considered. But on using Bi=1, there exists a gradient along the thickness of the element and this is neglected. The approach approximates the convective heat transfer coefficient (h) to k/L. In future analysis h value may be calculated within the program for each element. This might bring the elemental approach results closer to FEMLAB results. The purpose of this investigation using 1-inch length is to compare the results with FEMLAB results and to setup a model for further studies of higher length of the conductor, change in flow parameters and heat transfer conditions. Although the square cross section of the conductor was approximated to a cylindrical conductor retaining the composite and water volumes the same in the elemental approach, the analysis results were used to understand the envelope for the best possible cooling.

This approach was extended to a conductor length of 67 m (maximum length of the modular coil used in QPS) and for more length of time. The results are presented below. The temperature distribution in the conductor as a function of time for different flow velocities of 1, 2, 3, 4 and 5 m/s was calculated at different points along the conductor lengths (inlet i.e., 0% length, 20%, 40%, 60%, 80% and at exit i.e., full length). The number of elements used in this analysis was 10,000. Sensitivity analysis revealed that results using 67,000 elements were almost identical to those obtained using 10,000 elements. The maximum change in temperature value observed was only $0.1^{o}C$ but it tremendously reduced the processing time from approximately 3 hours to ½ hour for 2 m/s flow velocity.

Fig. 5.9 shows the temperature distribution over time for the inlet element for different velocities. Since there is a little difference of around $0.1^{o}C$, 5 curves overlap to be seen as 1. The inlet element cools to around $22^{o}C$ in 100 s.

Fig. 5.10 shows the Temperature distribution as a function of time at 20% length (2000^{th} element) of the conductor. At the end of 5 min, 5 m/s flow showed a difference of $8^{o}C$ fall compared to 1 m/s flow.

Fig. 5.11 shows the Temperature versus time plot for 4000^{th} element. The curves are very close for the initial fall of $4^{o}C$ under 10 s. This is because the tube was filled with water initially (at t=0). So for the 1^{st} time step, the heat lost by all the elements were equal.

Fig. 5.12 shows the Temperature versus time plot for 6000^{th} element. As expected the cooling rate reduces with increase in length of the conductor. This is because the water elements pick heat on their way to the exit. This causes the difference in temperature (ΔT) between the conductor element and the water element to reduce, which in turn reduces the heat transfer.

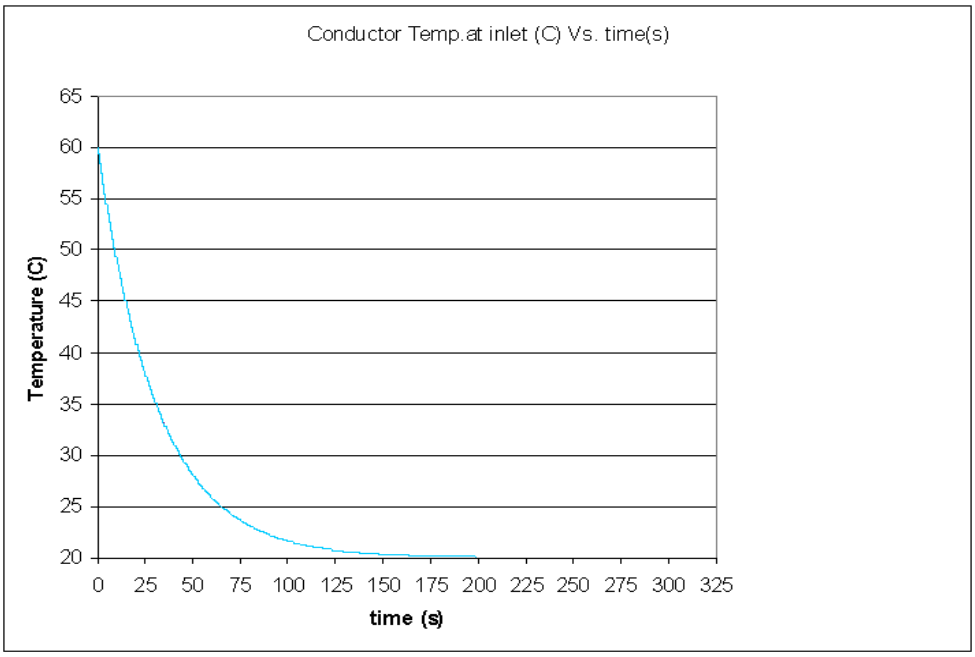

Fig. 5.9: Inlet Temperature-time plot (L=67m, v=1, 2, 3, 4, 5 m/s). 5 curves more or less overlap. Hence in this plot it's seen as a single curve.

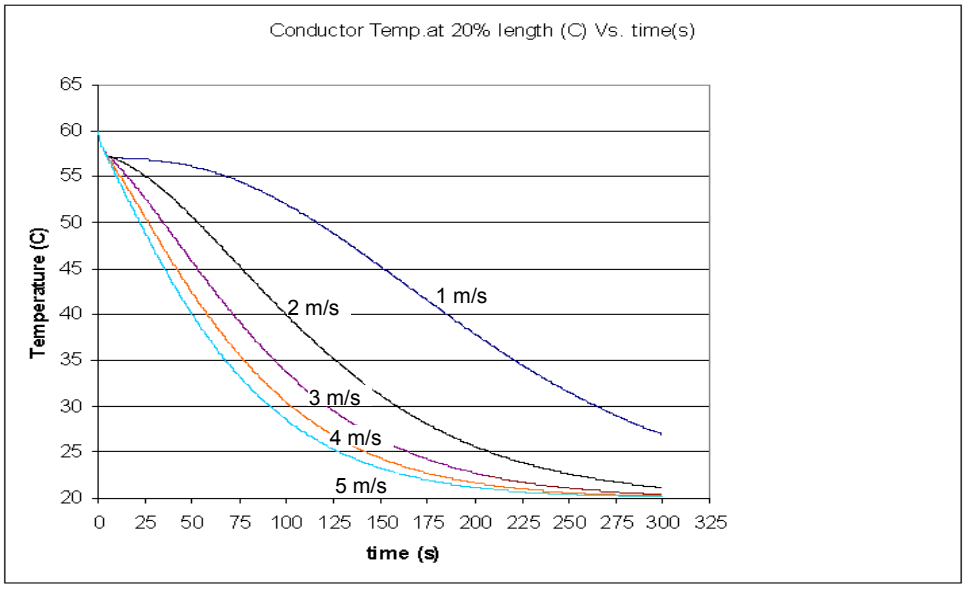

Fig. 5.10: 20% length Temperature-time plot (L=67m, v=1, 2, 3, 4, 5 m/s). These plots represent the bulk temperature value of the 2000th element in the tube starting from inlet.

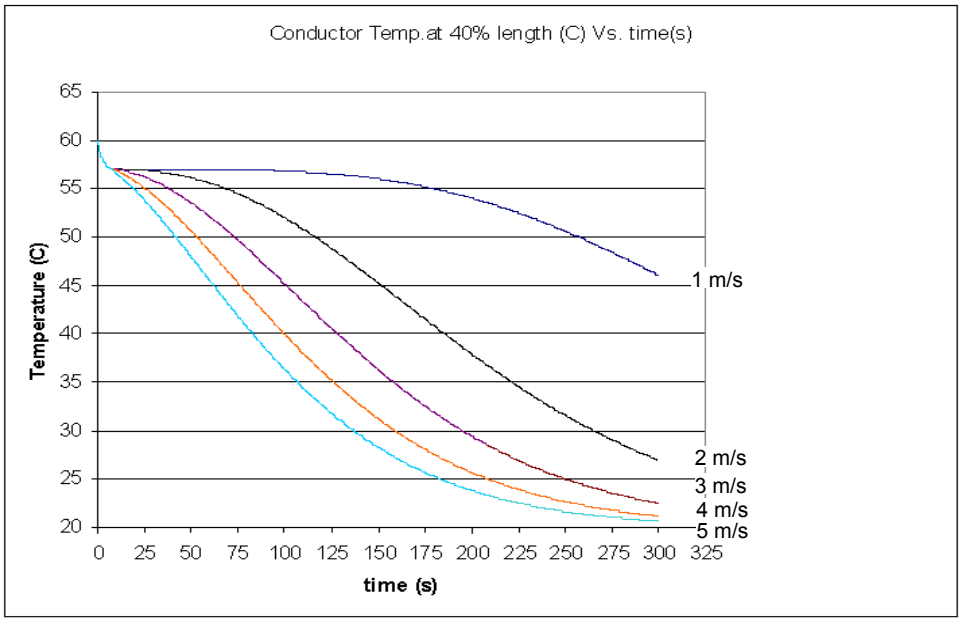

Fig. 5.11: 40% length Temperature-time plot (L=67m, v=1, 2, 3, 4, 5 m/s). There is an overlap by the curves during the initial few time steps. Because the tube is filled with water at start, the heat lost to the water in the first time step is equal for all elements.

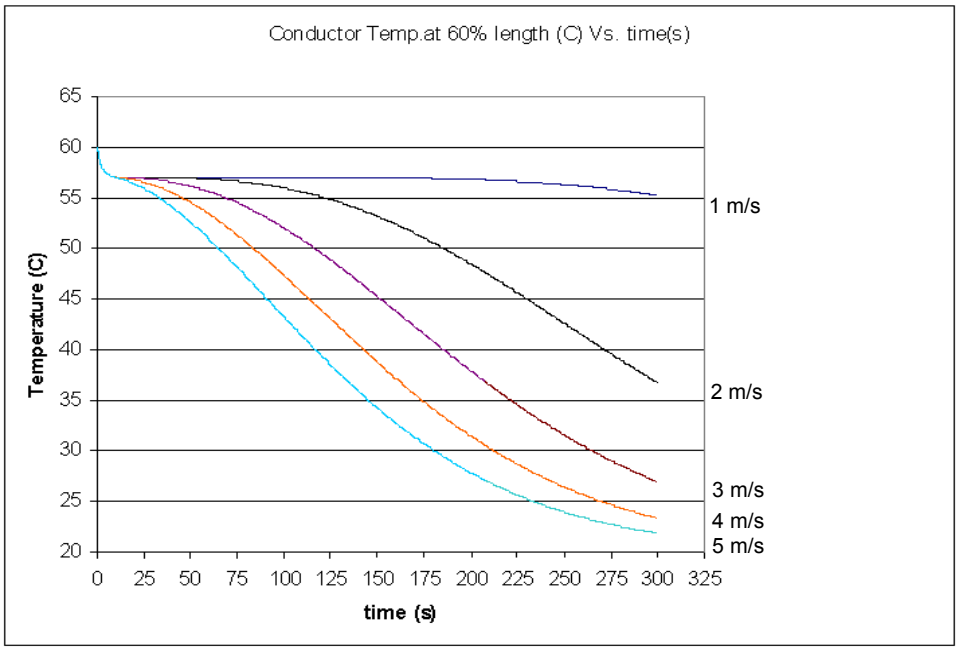

Fig. 5.12: 60% length Temperature-time plot (L=67m, v=1, 2, 3, 4, 5 m/s)

Fig. 5.13 plots the Temperature versus time of 8000th element. It may be noticed that at this length (53.6 m) the heat removed by water at 1 m/s is very minimal and hence the curve becomes almost a straight line.

Fig. 5.14 plots the Temperature distribution of the last (10,000th) element. The temperature values are highest here compared to earlier figures. This is because the elements that cross this length have already picked up enough heat to reduce ΔT.

Fig. 5.15 shows the Temperature versus time plot for all the water elements that cross the exit. It may be noted that for 1 m/s flow, the exit water element after the initial drop is almost at 57^{o}C up to 5 min.

Fig. 5.16 shows the temperature along length of the conductor at the end of 5 min. 5 m/s flow cools faster and most part (80% length) of the conductor is below 25^{o}C.

Fig. 5.17 shows the Temperature of water along the length at the end of 5 min. So from the plots it obvious that increased flow velocity cools the conductor much faster.

While it was clear that higher water velocity produced faster cooling, high water velocity will require a high pressure to force the water through a small diameter and long copper tubes. Another parameter that will produce faster cooling of composite conductor is the inlet water temperature. Hence analyses were carried using water at inlet Temperatures of 0^{o}C and 10^{o}C to understand the trade off between higher velocity flow at 20ºC and lower velocity flow at 10^{o}C. Temperature versus time results was plotted at different lengths (Fig. 5.18) along the conductor for a flow velocity of 2 m/s. It may be noticed that for 2 m/s velocity, when the inlet water temperature is reduced to 10ºC, the temperature at 40% length falls to nearly 19ºC compared to 27ºC when the inlet water temperature is 20ºC.

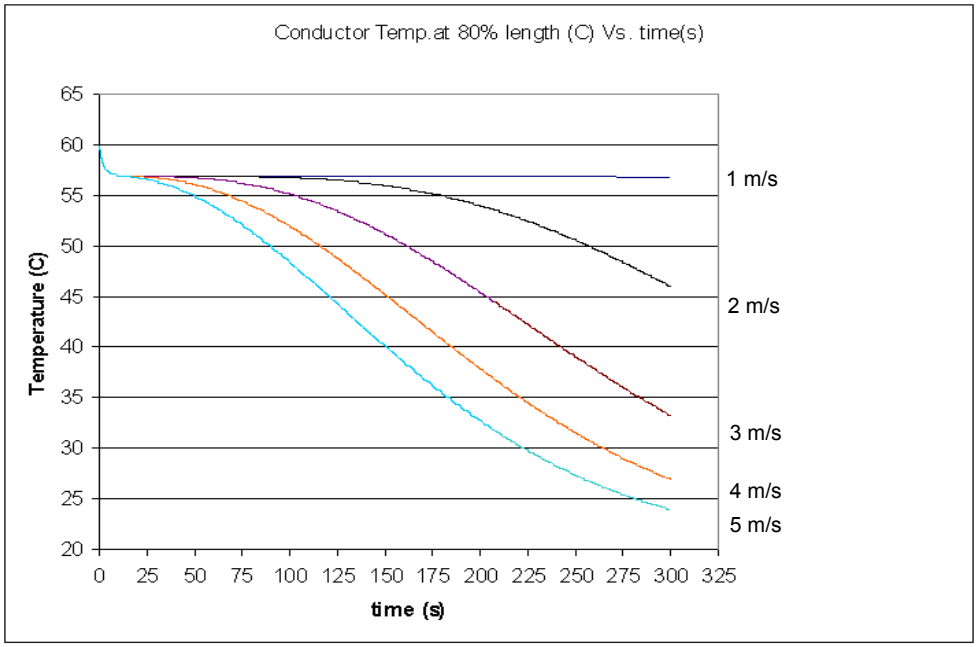

Fig. 5.13: 80% length Temperature-time plot (L=67m, v=1, 2, 3, 4, 5 m/s)

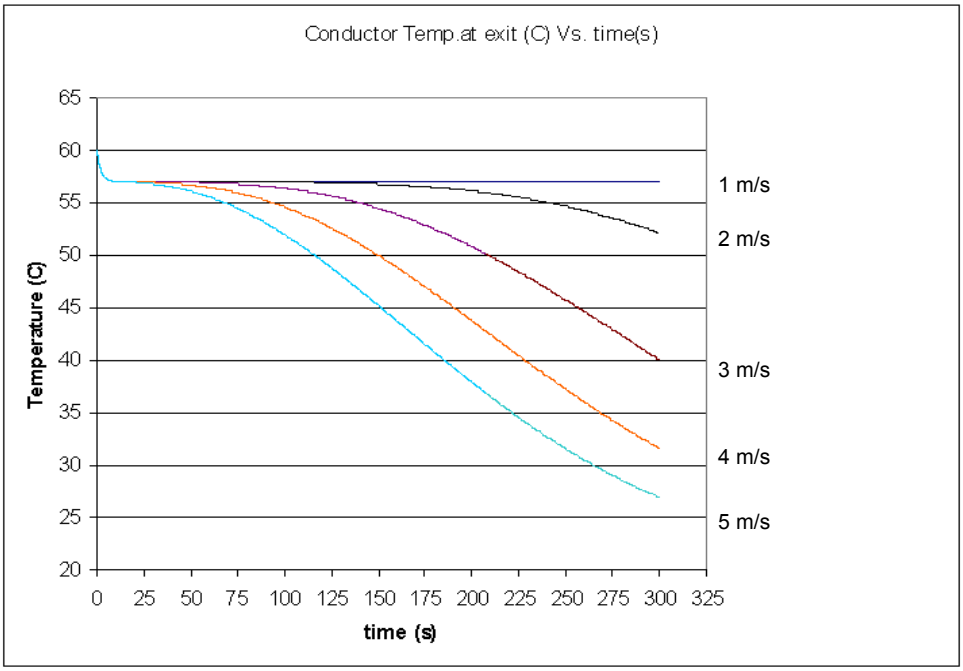

Fig. 5.14: Exit Temperature-time plot (L=67m, v=1, 2, 3, 4, 5 m/s)

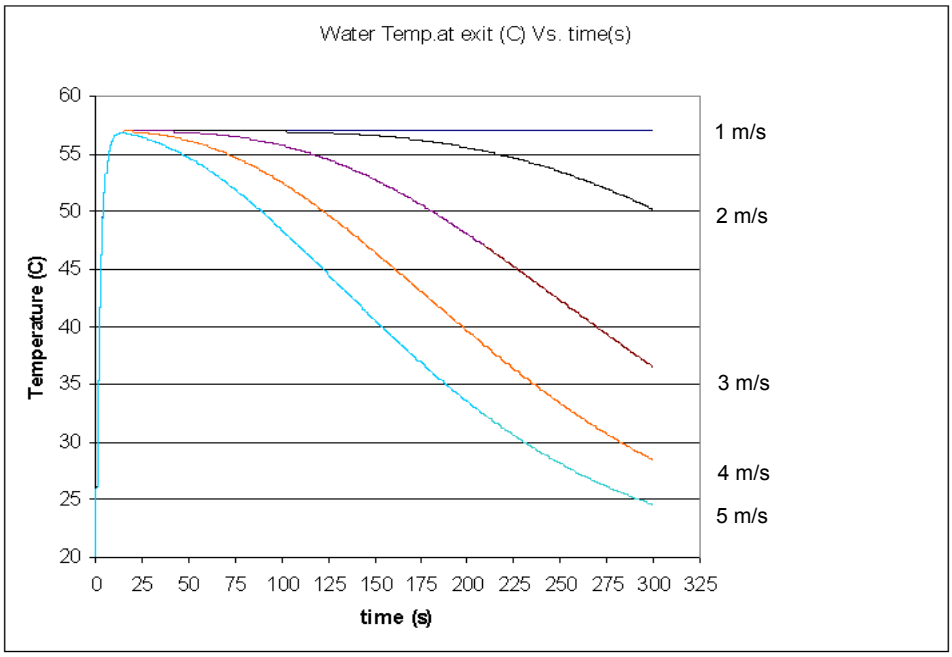

Fig. 5.15: Water exit Temperature-time plot (L=67m, v=1, 2, 3, 4, 5 m/s). The exit water Temperature for 1 m/s flow is close to 58ºC throughout. This explains the same temperature range for the exit composite element in Fig. 5.14 (1 m/s curve)

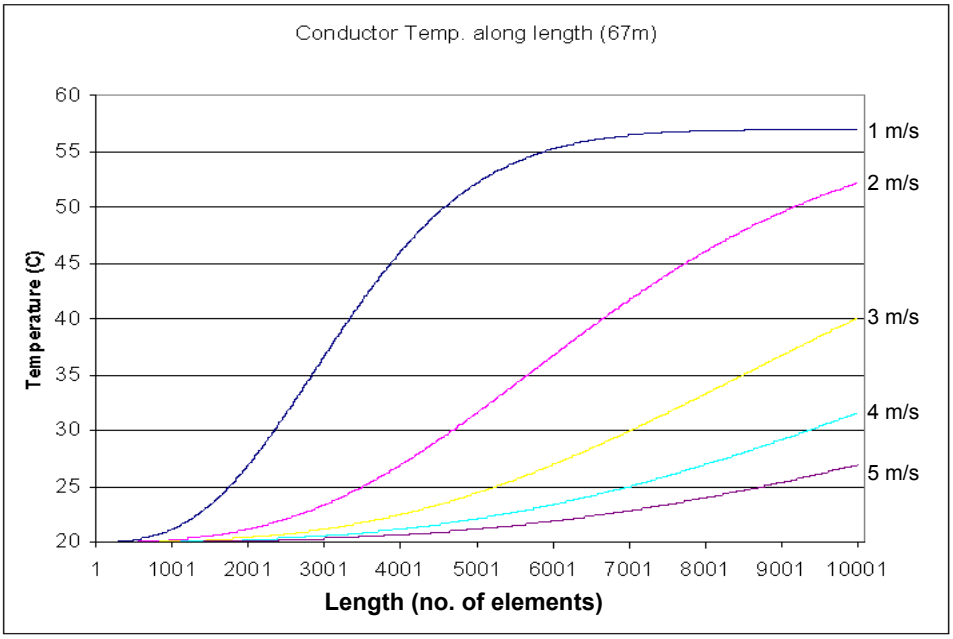

Fig. 5.16: Conductor Temperature at end of 5 min. (L=67m, v=1, 2, 3, 4, 5 m/s). Length is represented by the element numbers from 1 to 10,000.

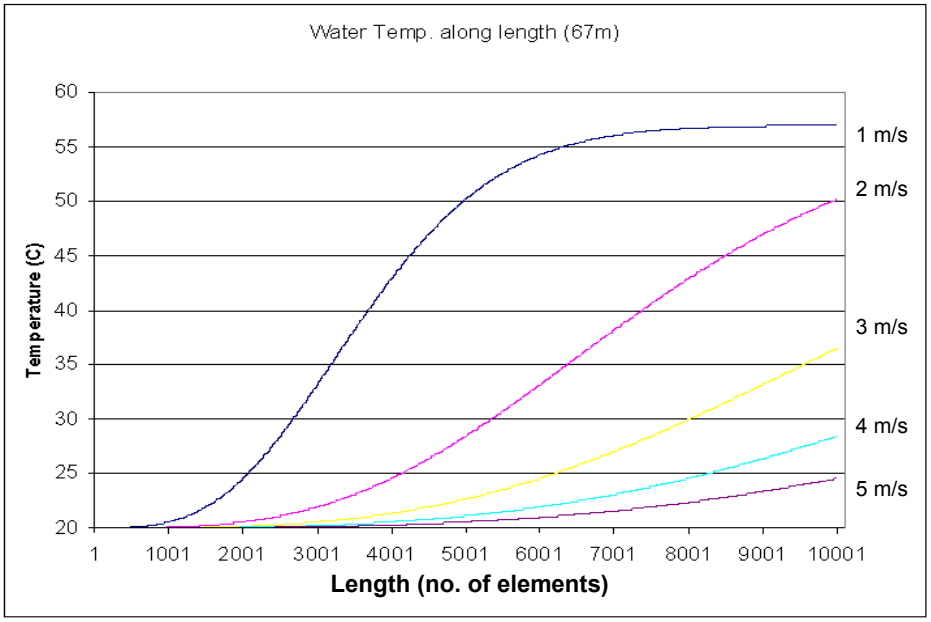

Fig. 5.17: Water Temperature at end of 5 min. (L=67m, v=1, 2, 3, 4, 5 m/s). Length is represented by the element numbers from 1 to 10,000.

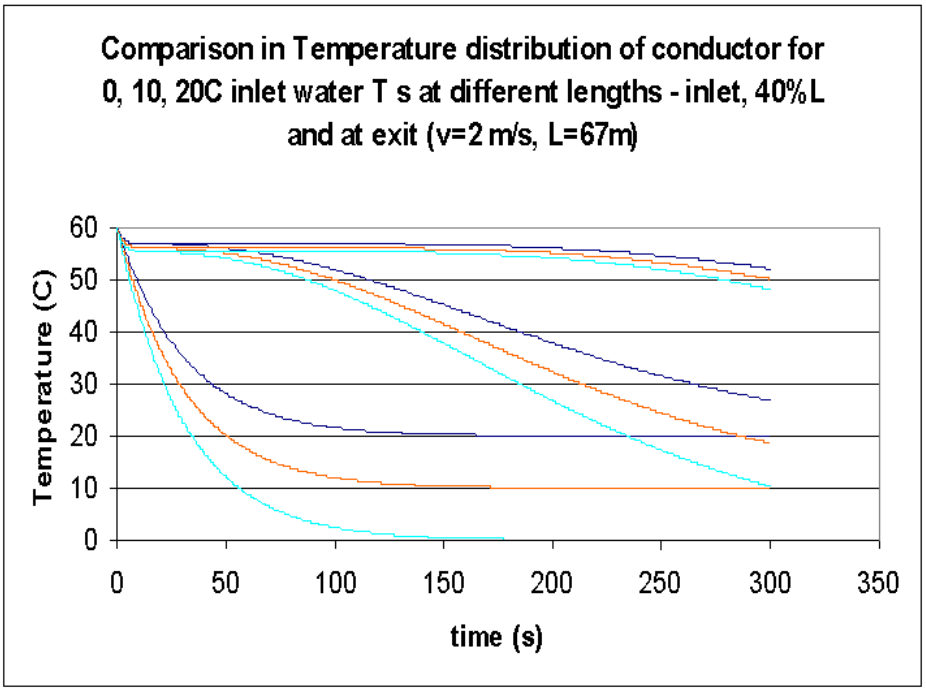

Fig. 5.18: Conductor Temperature for Inlet water T s= 0ºC, 10ºC & 20ºC. (L=67m, max t = 5 min, v = 2 m/s, Bi=1). Notice the 17°C difference at 40% length by the end of 5 min in comparison with 20ºC inlet.

At lesser tube lengths the temperature difference is still higher. This shows that reducing the inlet water temperature is effective and complements the cooling rate when used with higher water velocities.

Fig. 5.19 shows the conductor temperature as a function of time for very long time period. This analysis was carried over a 30 min time period and temperatures at different lengths were plotted. Inlet water temperature used was 20ºC.

The aforementioned results can be used to interpret the trend and approximate temperature distribution that might occur in the real conductor but the numerical values may not be exact because of the following 2 major reasons: 1) Axial conduction has been neglected in the development of the numerical model and 2) Biot number (Bi) has been assumed to be 1.

Since axial conductivity was neglected in the Elemental approach, the FEMLAB results were recomputed while assuming no axial conductivity. Fig. 5.20 shows a comparison of FEMLAB and Numerical results for 1-inch long conductor. Biot number used for this numerical approach was 1. For a practical velocity range of 1.5 – 2 m/s, the Biot number falls around 3. Fig. 5.21 shows a another comparison of FEMLAB and Numerical results for Biot number equal to 3. As can be seen that the difference between the FEMLAB and Elemental approach diminishes when a more realistic value of Biot number is used. The other major source that may be responsible for the difference between the FEMLAB and the Elemental analysis is that the later neglects transverse temperature gradient in the copper/polymer composite.

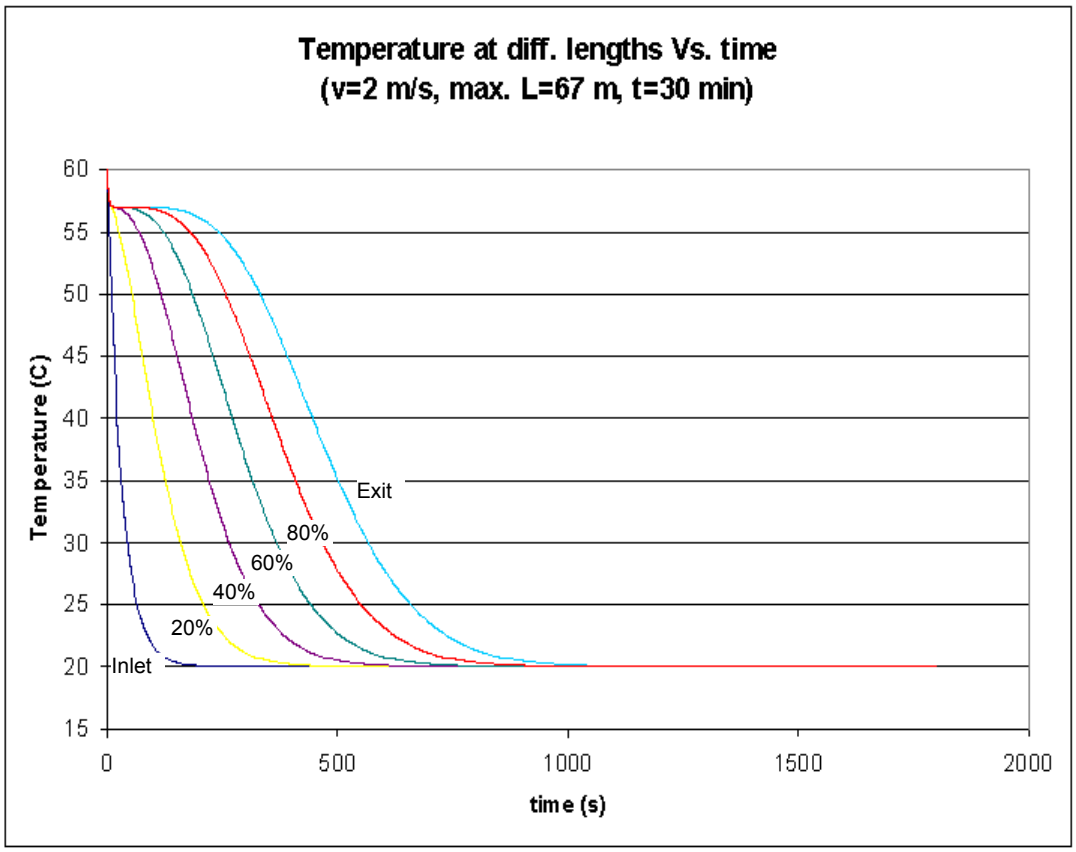

Fig. 5.19: Conductor Temperature Vs. time at 0, 20, 40, 60, 80, 100% lengths (L=67m, v=2 m/s). Entire tube cools in nearly 13 min.

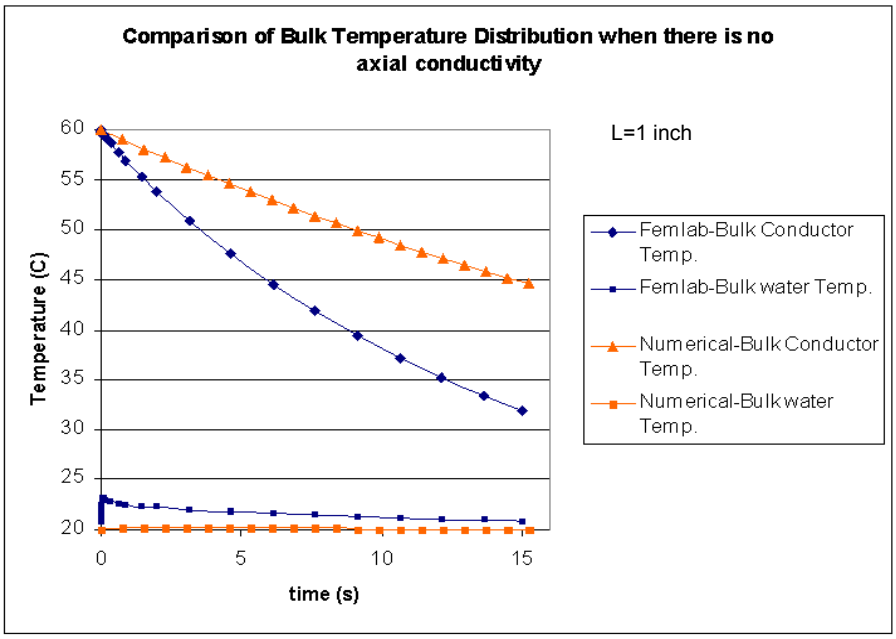

Fig. 5.20: Comparison between FEMLAB and Numerical results. Axial conductivity was neglected in both cases. Bi=1 for numerical approach. Note 13ºC difference at the end of 15s in the conductor.

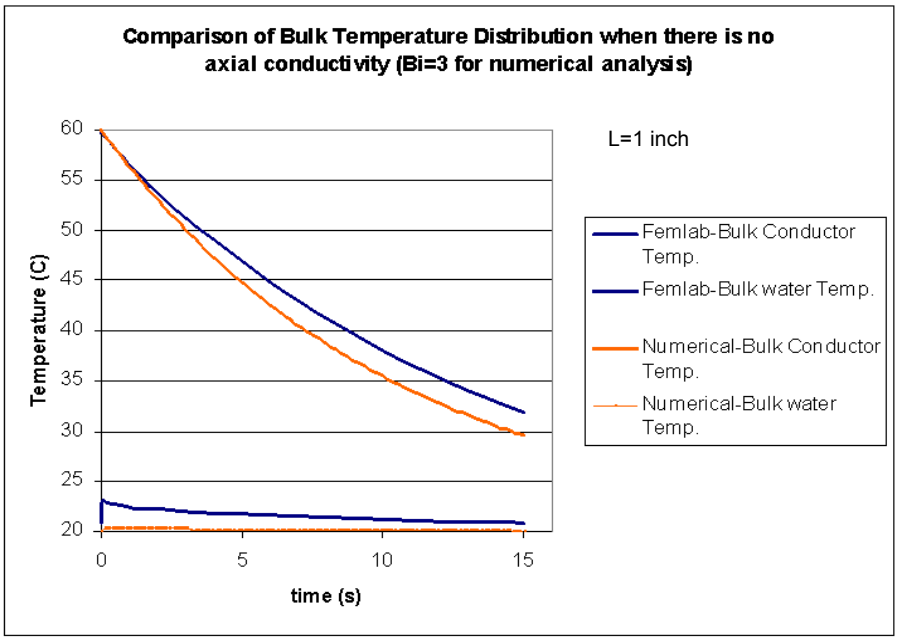

Fig. 5.21: Comparison between FEMLAB and Numerical results (Bi=3). Axial conductivity was neglected in both cases. Notice that cooling is more in numerical approach.

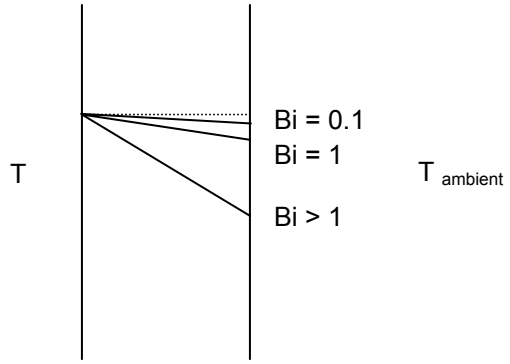

Fig. 5.22: Effect of Biot number on Temperature distribution at Steady state

5.3 SIGNIFICANCE OF BIOT NUMBER

Bi is a dimensionless number that gives the ratio of the resistance to conduction in the body to the resistance to convection. Bi assumed as 1, implies that the resistance to conduction and convection are equal. This may not be true because the resistance to convection is greater than resistance to conduction in real situations (Fig. 5.22).

Let $h = \frac{k}{L}$ (assumption)

Hence Bi = $\frac{hL}{k}$ = 1

r_2 = 0.005643326 m ; r_1 = 0.00162 m

Characteristic Length $L = \frac{r_2^2 - r_1^2}{2r_1}$ = 0.009019 m,

and *k* for the copper conductor in the radial direction is 12 W/m.K

h = 1330.471 W/m^2.K for the above assumption.

Table 5.2: Comparison of Bi=1 and Bi=7 (Heisler chart values)

Description	c value for Bi = 1	c value for Bi = 7
Fo=0.03, t=1 s	0.99	0.99
Fo=0.3, t=10 s	0.8	0.55
Fo=3, t=100 s	0.012	~ 0

But for practical applications the convective heat transfer coefficient of water is approximately 10,000 W/m^2.K. The effect of this increased numerical can be understood from the heat transfer equation

$$\frac{q}{A} = \frac{T_i - T_0}{(\frac{L_a}{k_a} + \frac{1}{h_0})}$$ for a plane wall (h_o is the convective coefficient)

So in a pure conduction problem the heat transferred will be more than when a convective heat transfer coefficient exists.

When a higher value of h such as 10,000 W/m^2.K is used, the Biot number might increase 7 to 8 times. Table 5.2 helps in understanding the implications of a higher Biot number. Table 5.2 was built by using Heisler chart [23].

Fourier number (F_o) can be calculated from characteristic length and time. $T_0 = c(T_i - T_{ambient}) + T_{ambient}$ where c is a constant obtained from Heisler chart.

The difference $(T_i - T_{ambient})$ may be assumed 40^{o}C maximum. (Initial temperature of the conductor is 60^{o}C and inlet water temperature is 20^{o}C).

From the above table, at t=10s,

T_0 = 23.2^{o}C for Bi = 1 and T_0 = 22.2^{o}C for Bi = 7.

From the above it can be noticed that the effective change in temperature is 1^{o}C, which is trivial for the problem in hand.

At t=100s,

T_0 = 20.4^{o}C for Bi = 1 and T_0 = 20^{o}C for Bi = 7.

After 100s for a maximum ΔT value of 40^{o}C, the difference in temperature for Bi=1 and Bi=7 is only 0.4 ^{o}C. Hence it may be concluded that a deviation in Biot number from 1 (which is used in the model) to 7 (for a more practical heat transfer coefficient h) does not greatly effect the cooling time.

6. CONCLUSIONS

6.1 FILLING AND FLUSHING OF THE 200-ft SOFT ANNEALED COPPER TUBE

Based on lessons learnt from the experimental methodology used for filling and flushing the tube and weight/flow measurement results, significant process improvement was achieved. An efficient and cleaner means of filling/flushing 200-ft long soft annealed copper was developed. The following conclusions were reached in this regard:

- Pre-coating the inner wall of the copper tubes with silicone oil, handling the molten cerrobend under silicone oil without exposure to air, using double boiler for melting cerrobend to assure the temperature is always lower than 100^{o}C, cold water quenching of the filled tube at 10^{o}C (50^{o}F), and flushing the tube with hot water under pressure are some key measures implemented in the improved process.
- Cerrobend was identified as the most suitable Low Melting Alloy given its physical/thermal properties and ease of handling.

6.2 CTD-403 STUDY

- Flexural Modulus values of CTD-403 specimens were obtained from bend tests.
- Test coil was developed at MDL to understand the cure cycle behavior of CTD-403, to get hands-on experience in conductor lay-up and to learn the intricacies in filling the copper conductor coil with CTD-403 by Vacuum Pressure Impregnation (Section 3.8).

6.3 HEAT TRANSFER ANALYSIS

- A numerical model to analyze the cooling rate in the 200-ft long conductor was developed with some approximations.
- The temperature distribution in the composite conductor and in flowing water was calculated using the model and the FEMLAB. The comparison of the results from the two

methods showed that while the there was a difference in numerical values, the trends in the temperature plots were similar.

- In this model, the convective heat transfer coefficient (h) may be readily introduced to simulate the real time condition.
- Parametric studies may be easily conducted for any future change in physical or thermal conditions. For example – different flow velocities of the cooling water, change of cooling medium – which needs change of property values, change in dimensions or properties of the conductor or the tube, initial temperature of the conductor or coolant etc.
- The analysis results provide an upper bound for the cooling rate i.e. the maximum cooling that can be expected in the conductor coil in a given time.
- Although this model provides an upper bound of the maximum possible cooling, the cooling time predicted in this model will not greatly differ from the application. This may be understood from the fact that an increase in Biot number to 7 (for a more practical h) causes a difference of $1^{o}C$ from the model for a difference in temperature (ΔT) value of $40^{o}C$ after 10 seconds. This is not of much engineering significance. In the real application, ΔT value keeps reducing as each element moves picking heat from the inlet to exit.

7. FUTURE WORK

7.1 FINITE ELEMENT MODELING

- Copper tube may be introduced in the finite element model instead of approximating the tube to a hole in the conductor, which carries the cooling water (Fig. 4.1). Because copper has very high conductivity compared to the composite in radial direction (33 times), cooling rate would be improved.
- Use of commercial version of FEMLAB software would allow the user to increase the length of the model from 1-inch and use higher number of elements for meshing. This would validate the results of the approximate model for long tube.
- Experiments should be conducted to predict the exact thermal conductivity of the composite conductor in the radial direction. This value may be used in the model.
- The exact value of specific heat of the composite may be determined through experiments.

7.2 ELEMENTAL APPROACH

- Axial conductivity between the elements should be incorporated. This would be an important step ahead in the existing model because the axial conductivity would be as high as conductivity of copper (~400 W/m.K).
- Temperature gradient may be introduced in the model instead of using the bulk temperatures of elements. This would change the Biot number used.
- The accuracy of the model could be improved by calculating a convective heat transfer coefficient. This value could be used in calculating the heat lost by the composite element to the water element.
- If the use of bulk temperature of elements is continued, the number of elements in the radial direction could be increased to take the model closer to the existence of a radial temperature gradient.

- Copper tube may be introduced in the model (as in 7.1).
- Exact value of the radial conductivity and specific heat of the composite may be determined through experiments and used in the model (as in 7.1).
- The predicted results should be verified by controlled laboratory experiments.

REFERENCES

1. K.D. Freudenberg, P. Goranson and F. Dahlgren, Cooling design and analysis of the QPS modular coil winding packs, 21st IEEE/NPSS Symposium On Fusion Engineering, (2005).
2. http://www.eia.doe.gov/neic/press/press235.html
3. C.W. Leung and S. D. Probert, Applied Energy, 50, 313 (1995).
4. C.W. Leung and S. D. Probert, Applied Energy, 57, 13 (1997).
5. G. Wang and S.P. Vanka, International Journal of Heat and Mass Transfer, 38, 3219 (1995).
6. Yauo Mori and Wataru Nakayama, International Journal of Heat and Mass Transfer, 10, 1179 (1967).
7. X. Lu, P. Tervola, M. Viljanen, International Journal of Heat and Mass Transfer, 49, 341 (2006).
8. X. Lu, P. Tervola, M. Viljanen, International Journal of Heat and Mass Transfer, 49, 1107 (2006).
9. E.K. Kalinin and G.A. Dreitser, International Journal of Heat and Mass Transfer, 28, 361 (1985).
10. Yuzhi Sun and Indrek S. Wichman, International Journal of Heat and Mass Transfer, 47, 1555 (2004).
11. F. de Monte, International Journal of Heat and Mass Transfer, 43, 3607 (2000).
12. Abram Dorfman, Journal of Heat Transfer, 126, 149 (2004)
13. http://hitechalloys.com/hitechalloys_005.htm
14. http://canadametal.com/pdf/cerro_bending.pdf
15. Madhukar, Shankar, Joe Campbell, Magnet Development Laboratory (MDL) minutes – May 20, 2005 (http://web.utk.edu/~qps/meeting_notes/notes.html).
16. M. Madhukar, S. Narasimhaswami and Robert Benson, Conductor R&D for QPS, 21st IEEE/NPSS Symposium On Fusion Engineering, (2005).

17. Goranson, Madhukar, and Benson, Magnet Development Laboratory (MDL) minutes – Nov 22, 2005.
18. Benson, Magnet Development Laboratory (MDL) minutes – Dec 20, 2005.
19. Benson, Magnet Development Laboratory (MDL) minutes – Jun 21, 2006.
20. Private discussions with Mr. Paul Goranson, Magnet Development Lab.
21. Donald Pitts and Leighton Sissom, Heat Transfer, Schaum's Outlines, 1998.
22. B Sundqvist et.al., Journal of Applied Physics, 10, 1397 (1977).
23. Frank P. Incropera and David P. Dewitt, Fundamentals of Heat and Mass transfer, John Wiley and Sons, 1990.
24. I Kaban et.al., Journal of Physics: Condensed matter, 16, 6335 (2004).
25. B. E. Nelson et.al., Fusion Technology, IAEA (2005).
26. Wayne C. Weyer et.al., 46th AIAA Structures, Structural Dynamics and Materials Conference (2005).
27. http://web.utk.edu/~qps

APPENDIX

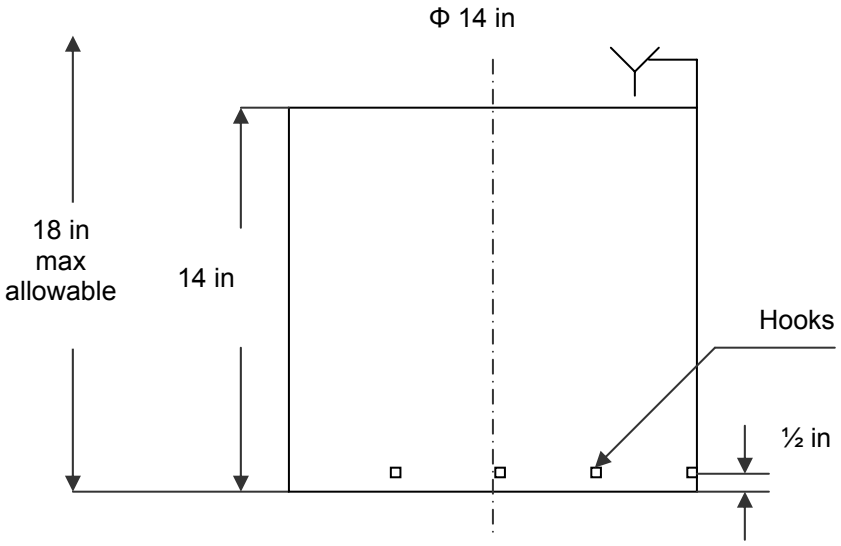

Fig. A.1: Dimensions of the spool used for winding 200 feet Copper tube. The maximum available height was 18 inches because the height was restricted by the oven dimensions. Blue M Metric – Stabil Therm oven with a maximum range of 250ºC was used.

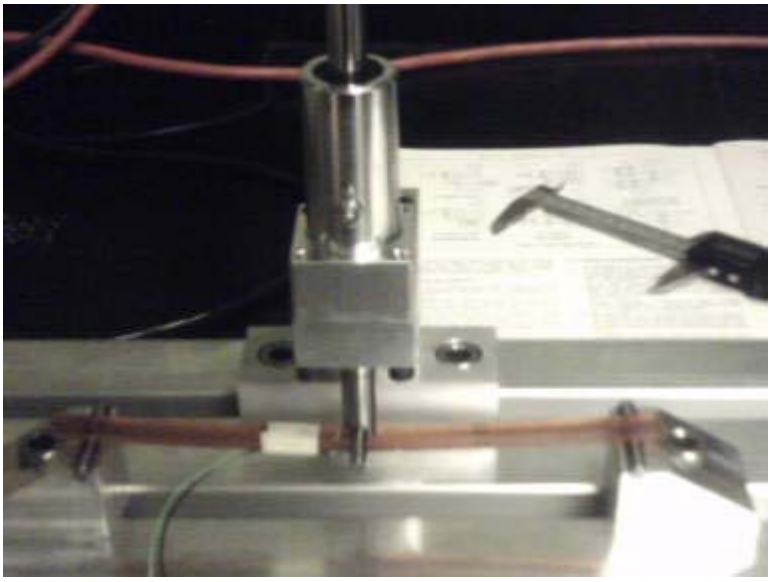

Fig. A.2: Bend tests on CTD 403 specimen. Refer Section 3.7.

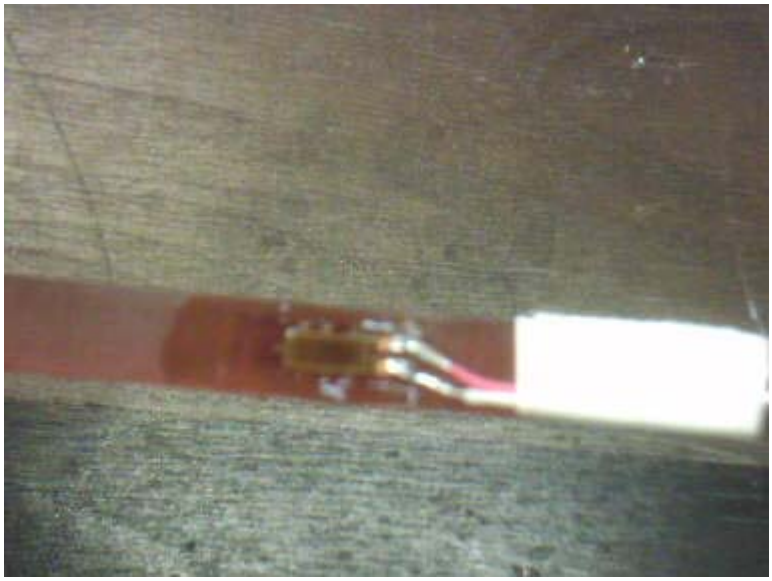

Fig. A.3: Close-up view of the strain gauge glued to the CTD 403 specimen before bend test. The leads connect to the strain gage amplifier (Section 3.7).

The following is the MATLAB code developed for analysis using the elemental approach as explained in Section 4.4.

```
% HEAT TRANSFER ANALYSIS OF QPS COIL%

% ELEMENTAL APPROACH %
clc
clear all
% Lumped system analysis
% All units in SI system, Temperature in Celcius scale.

% ---- User defined variables ----
v = 2; % Velocity of water in m/s
length_of_tube = 67; % in m
time_of_result = 300; % in seconds. Result wanted at end of this time period.
n = 10000; % number of elements in the model
Bi = 1; % Biot number

Excel = actxserver('Excel.Application');
set(Excel, 'Visible', 1);
% Insert a new workbook
Workbooks = Excel.Workbooks;
Workbook = invoke(Workbooks, 'Add');


start_time = cputime ;
% calculation of time step for the given no. of elements
t_inlet_to_outlet = length_of_tube/v ;
t = t_inlet_to_outlet/n ;

   % ---- User Print screen data ----
   sprintf ('Length of tube considered = %.2f m.',length_of_tube)
   sprintf ('Velocity of water = %.2f m/s',v)
   sprintf (Biot number = %.1f ',Bi)
   sprintf ('Temperature distribution required at time = %.3f seconds',time_of_result)
   sprintf ('Number of elements used in the model = %.0f ',n)
   sprintf ('Time step used in the model = %.8f ',t)

         % ---- Property Values ---------
         k = 12; % Conductivity of Composite 12 W/m-K
         Tcomposite = 60; % Initial temp of Cu composite -- provided later as Tc
         Twater_inlet = 20;  % Initial temp of water -- provided later as Tw
         rho = 6705; %density of composite in Kg/m3
         Cp = 688; % Specific heat in SI J/kg-K
         rho_w = 1000; %density of water
         Cpw = 4200; %Specific heat of water

         % -----Geometry of tube ------------
   % Model assumes cylindrical conductor
         ro = 0.005643326;% Outside diameter in m. Caculated for Equivalent volume of the
square conductor.
         ri = 0.003239/2; %inside diameter in m
         L= (ro^2 - ri^2) / (2*ri) ;% Effective length calculated from Volume / Surface Area
         Fo = k/(rho*Cp) * t/L^2; % Fourier number
```

```
        Tc(1:n)=Tcomposite; % intial temperature of composite in C
        Tw(1:n) = Twater_inlet;

        count = 1;
          for time=t:t:time_of_result

      for i=1:n
         Tcafter(i) = ((Tc(i)-Tw(i)) * exp(-Bi*Fo)) + Tw(i);
         Twafter(i) = Tw(i) + ( (ro^2-ri^2)*rho*Cp*( Tc(i)-Tcafter(i)))/(ri^2*rho_w*Cpw);
      end
      T_inlet_element_Cu(count)=Tcafter(1);
      T_mid2000_element_Cu(count)=Tcafter(.2*n);
      T_mid4000_element_Cu(count)=Tcafter(.4*n);
      T_mid6000_element_Cu(count)=Tcafter(.6*n);
      T_mid8000_element_Cu(count)=Tcafter(.8*n);
      T_outlet_element_Cu(count)=Tcafter(n);

      T_outlet_element_water(count)=Twafter(n);

      Tc = Tcafter;
      Twintermediate = Twafter;
      Twintermediate = Twintermediate( 1:(n-1) );
      Twnew=[Twater_inlet,Twintermediate];
      Tw=Twnew;

      time_steps(count)=time;
      T_bulk_Cu(count) = sum(Tcafter)/length(Tcafter) ;
      T_bulk_w(count) = sum(Twafter)/length(Twafter);
      count = count + 1;

    end


  if  time_of_result - time > 0
      sprintf ('Temperature distribution was calculated at %.3f seconds.\nTemperature distribution
was requested at %.3f seconds.\nTo calculate at the exact time, please increase the number of
elements.',time,time_of_result)
  end

    figure(1);
    subplot(4,1,1); plot(Tcafter) %composite T along length
    subplot(4,1,2); plot(Twafter) %water T along length

    subplot(4,1,3); plot(time_steps,T_bulk_Cu) % Bulk temp of cu vs. time
    subplot(4,1,4); plot(time_steps,T_bulk_w) %Bulk temp of water vs. time

    figure(2)
    subplot(7,1,1); plot(time_steps,T_inlet_element_Cu) %inlet cu temp vs. time

    subplot(7,1,2); plot(time_steps,T_mid2000_element_Cu) % 20% length element T as f(t)
    subplot(7,1,3); plot(time_steps,T_mid4000_element_Cu) % 40% length element
    subplot(7,1,4); plot(time_steps,T_mid6000_element_Cu) % 60% length element
    subplot(7,1,5); plot(time_steps,T_mid8000_element_Cu) % 70% length element
```

```
subplot(7,1,6); plot(time_steps,T_outlet_element_Cu) %outlet cu temp vs.time
subplot(7,1,7); plot(time_steps,T_outlet_element_water) %outlet water temp vs.time

% To get data in excel%%

time_steps_excel = time_steps(1:100:end);
T_inlet_element_Cu_excel=T_inlet_element_Cu(1:100:end);
T_mid2000_element_Cu_excel=T_mid2000_element_Cu(1:100:end);
T_mid4000_element_Cu_excel=T_mid4000_element_Cu(1:100:end);
T_mid6000_element_Cu_excel=T_mid6000_element_Cu(1:100:end);
T_mid8000_element_Cu_excel=T_mid8000_element_Cu(1:100:end);
T_outlet_element_Cu_excel=T_outlet_element_Cu(1:100:end);
T_outlet_element_water_excel=T_outlet_element_water(1:100:end);
T_bulk_Cu_excel=T_bulk_Cu(1:100:end);
T_bulk_w_excel=T_bulk_w(1:100:end);

        % Make the 1st sheet active
        Sheets = Excel.ActiveWorkBook.Sheets;
        sheet_v = get(Sheets, 'Item', 1);
        invoke(sheet_v, 'Activate');
        % Get a handle to the active sheet
        Activesheet = Excel.Activesheet;
        % Put a MATLAB array into Excel
        ActivesheetRange = get(Activesheet,'Range','A1');
        set(ActivesheetRange, 'Value', 'time steps(s)');
        ActivesheetRange = get(Activesheet,'Range','A2:A44780');
        set(ActivesheetRange, 'Value', time_steps_excel(:));


        ActivesheetRange = get(Activesheet,'Range','B1');
        set(ActivesheetRange, 'Value', 'Cu inlet Temp.(C)');
        ActivesheetRange = get(Activesheet,'Range','B2:B44780');
        set(ActivesheetRange, 'Value', T_inlet_element_Cu_excel(:));

        ActivesheetRange = get(Activesheet,'Range','C1');
        set(ActivesheetRange, 'Value', 'Cu 20% Temp.(C)');
        ActivesheetRange = get(Activesheet,'Range','C2:C44780');
        set(ActivesheetRange, 'Value', T_mid2000_element_Cu_excel(:));

        ActivesheetRange = get(Activesheet,'Range','D1');
        set(ActivesheetRange, 'Value', 'Cu 40% Temp.(C');
        ActivesheetRange = get(Activesheet,'Range','D2:D44780');
        set(ActivesheetRange, 'Value', T_mid4000_element_Cu_excel(:));

        ActivesheetRange = get(Activesheet,'Range','E1');
        set(ActivesheetRange, 'Value', 'Cu 60% Temp.(C)');
        ActivesheetRange = get(Activesheet,'Range','E2:E44780');
        set(ActivesheetRange, 'Value', T_mid6000_element_Cu_excel(:));

        ActivesheetRange = get(Activesheet,'Range','F1');
        set(ActivesheetRange, 'Value', 'Cu 80% Temp.(C)');
        ActivesheetRange = get(Activesheet,'Range','F2:F44780');
        set(ActivesheetRange, 'Value', T_mid8000_element_Cu_excel(:));

        ActivesheetRange = get(Activesheet,'Range','G1');
```

```
set(ActivesheetRange, 'Value', 'Cu exit Temp.(C)');
ActivesheetRange = get(Activesheet,'Range','G2:G44780');
set(ActivesheetRange, 'Value', T_outlet_element_Cu_excel(:));

ActivesheetRange = get(Activesheet,'Range','H1');
set(ActivesheetRange, 'Value', 'Water exit Temp.(C)');
ActivesheetRange = get(Activesheet,'Range','H2:H44780');
set(ActivesheetRange, 'Value', T_outlet_element_water_excel(:));

ActivesheetRange = get(Activesheet,'Range','I1');
set(ActivesheetRange, 'Value', 'Cu Temp. along length(C)');
ActivesheetRange = get(Activesheet,'Range','I2:I10001');
set(ActivesheetRange, 'Value', Tcafter(:));

ActivesheetRange = get(Activesheet,'Range','J1');
set(ActivesheetRange, 'Value', 'Water Temp. along length(C)');
ActivesheetRange = get(Activesheet,'Range','J2:J10001');
set(ActivesheetRange, 'Value', Twafter(:));

ActivesheetRange = get(Activesheet,'Range','K1');
set(ActivesheetRange, 'Value', 'Cu bulk Temp. with time(C) ');
ActivesheetRange = get(Activesheet,'Range','K2:K44780');
set(ActivesheetRange, 'Value', T_bulk_Cu_excel(:));

ActivesheetRange = get(Activesheet,'Range','L1');
set(ActivesheetRange, 'Value', 'Water bulk Temp. with time(C) ');
ActivesheetRange = get(Activesheet,'Range','L2:L44780');
set(ActivesheetRange, 'Value', T_bulk_w_excel(:));

ActivesheetRange = get(Activesheet,'Range','M1');
set(ActivesheetRange, 'Value', 'RESULTS FOR VELOCITY=2m/s,67m ');

% Now save the workbook
invoke(Workbook, 'SaveAs', 'RESULTS FOR VELOCITY=2m/s,67m');

total_time = cputime - start_time;
sprintf ('Actual running time of the model %.4f  minutes.',(total_time/60) )
```

% END OF CODE

VITA

Shankar Narasimhaswami was born on January 13th, 1981 in Coimbatore, an industrial city in Southern India. He pursued his Bachelor's in Mechanical Engineering at PSG College of Technology, Coimbatore (www.psgtech.edu). Upon completion he moved to Trivandrum, India and then to Bombay, India to work for TATA Consultancy Services (www.tcs.com), a software firm. Later he moved to University of Tennessee, Knoxville, USA (www.utk.edu) in the Fall of 2004 to start a graduate study in Mechanical Engineering. While pursuing his Master's, he worked as a Graduate Research Assistant at the Innovative Computing Lab, Department of Computer Science, UT (http://icl.cs.utk.edu) for a year. By Spring of 2005 he started working as Graduate Research Assistant for Dr. Madhu S. Madhukar at the Magnet Development Lab on the Quasi-Poloidal Stellarator project (http://web.utk.edu/~qps), which is jointly carried by the Oak Ridge National Lab researchers and UT engineers. He will be graduating in December 2006 and will be pursuing a graduate study in Statistics starting August 2006.